

1999

Absolute photoluminescence yield in color converters for organic light emitting diodes

Weijie Zhang
San Jose State University

Follow this and additional works at: https://scholarworks.sjsu.edu/etd_theses

Recommended Citation

Zhang, Weijie, "Absolute photoluminescence yield in color converters for organic light emitting diodes" (1999). *Master's Theses*. 1964.
DOI: <https://doi.org/10.31979/etd.8fmz-s6nw>
https://scholarworks.sjsu.edu/etd_theses/1964

This Thesis is brought to you for free and open access by the Master's Theses and Graduate Research at SJSU ScholarWorks. It has been accepted for inclusion in Master's Theses by an authorized administrator of SJSU ScholarWorks. For more information, please contact scholarworks@sjsu.edu.

INFORMATION TO USERS

This manuscript has been reproduced from the microfilm master. UMI films the text directly from the original or copy submitted. Thus, some thesis and dissertation copies are in typewriter face, while others may be from any type of computer printer.

The quality of this reproduction is dependent upon the quality of the copy submitted. Broken or indistinct print, colored or poor quality illustrations and photographs, print bleedthrough, substandard margins, and improper alignment can adversely affect reproduction.

In the unlikely event that the author did not send UMI a complete manuscript and there are missing pages, these will be noted. Also, if unauthorized copyright material had to be removed, a note will indicate the deletion.

Oversize materials (e.g., maps, drawings, charts) are reproduced by sectioning the original, beginning at the upper left-hand corner and continuing from left to right in equal sections with small overlaps.

Photographs included in the original manuscript have been reproduced xerographically in this copy. Higher quality 6" x 9" black and white photographic prints are available for any photographs or illustrations appearing in this copy for an additional charge. Contact UMI directly to order.

**Bell & Howell Information and Learning
300 North Zeeb Road, Ann Arbor, MI 48106-1346 USA**

UMI[®]
800-521-0600

**ABSOLUTE PHOTOLUMINESCENCE YIELD
IN COLOR CONVERTERS
FOR ORGANIC LIGHT EMITTING DIODES**

**A Thesis Presented to
The Faculty of the Department of Materials Engineering
San Jose State University**

**In Partial Fulfillment
of the Requirements for the Degree
Master of Sciences**

**By
Weijie Zhang
December, 1999**

UMI Number: 1397762

UMI[®]

UMI Microform 1397762

Copyright 2000 by Bell & Howell Information and Learning Company.

**All rights reserved. This microform edition is protected against
unauthorized copying under Title 17, United States Code.**

**Bell & Howell Information and Learning Company
300 North Zeeb Road
P.O. Box 1346
Ann Arbor, MI 48106-1346**

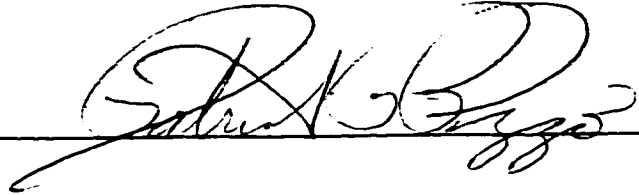
©1999

Weijie Zhang

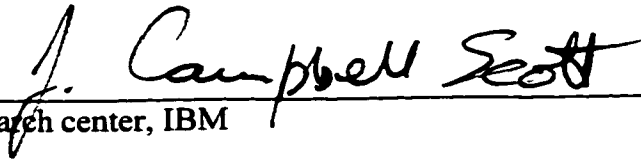
ALL RIGHTS RESERVED

APPROVED FOR THE DEPARTMENT OF MATERIALS ENGINEERING

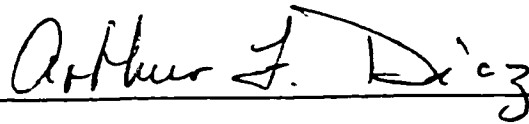
Professor Partrick Pizzo

A handwritten signature in cursive script, appearing to read "Partrick Pizzo", written over a horizontal line.

Dr. J. Campbell Scott, Almenden Research center, IBM

A handwritten signature in cursive script, appearing to read "J. Campbell Scott", written over a horizontal line.

Professor Art Diaz

A handwritten signature in cursive script, appearing to read "Arthur J. Diaz", written over a horizontal line.

APPROVED FOR THE UNIVERSITY

A handwritten signature in cursive script, appearing to read "William Fish", written over a horizontal line.

ABSTRACT

Absolute Photoluminescence Yield in color converters for Organic Light Emitting diodes

By weijie Zhang

The main focus of this thesis project is to develop a PL quantum efficiency measurement method for color converter thin film in OLED applications and to investigate the concentration effect of dye pair (Courmarin 334 with Pyrromethene 580) on the PL quantum efficiency for the two-dye system. The PL quantum efficiency was measured using a modified integrating-sphere method. The doping of a small amount of Pyrromethene 580 (0.1 wt%) into the host Courmarin 334 results in a twofold increase in PL quantum efficiency. The PL quantum efficiency of the two-dye system strongly depended on the concentration of Courmarin 334 but weakly on that of Pyrromethene 580. The two dye system has the maximum PL quantum efficiency when the concentration of Pyrromethene 580 is around 0.5% wt percent for a fixed concentration of C334. Based on the Forster energy transfer model, it is found 90% of the absorbed energy is released by the two competing mechanisms: Pyrromethene 580 radiative emission and Courmarin 334 non-radiative emission.

ACKNOWLEDGEMENTS

The fulfillment of this degree would not have been possible without the guidance and support from my advisors, Professor Patrick P. Pizzo and Dr. J. Campbell Scott, to whom I would like to express my great thanks and regards.

I would like to thank Jianping Chen for the help in this thesis work.

To my Parents

Table of Contents

LIST OF FIGURES	ix
LIST OF TABLES	xiii
1. THESIS OBJECTIVE	1
2. INTRODUCTION	2
3. BACKGROUND AND PRINCIPLES	3
3.1 Basic structure of an organic light emitting diode device	3
3.2 Progress in OLED development	6
3.3 Red, Green and Blue (RGB) form for creating full color	6
3.4 Suggested color tuning technology for OLEDs	9
3.4.1 Patterned emitters.....	9
3.4.2 Microcavities	9
3.4.3 Color filters	11
3.4.4 Stacked OLEDs	11
3.4.5 Fluorescent converters	11
3.5 The criterion for a good dye in a fluorescent converter system	12
3.5.1 High Purity of the desired color.....	12

3.5.2 High absorption of the incident light	13
3.5.3 High quantum efficiency of photoluminescence	15
3.6 External color conversion	16
3.6.1 Doped dye materials	16
3.6.2 Dye concentration effects.....	18
3.6.3 Energy transfer involved in the dye photoluminance (PL) process	21
3.6.4 A two-dye photoluminescence approach	24
3.7. A measurement method for the quantum efficiency	27
3.8 The modified PL quantum efficiency measurement	32
3.9 Environmental degradation of the color converter thin film.....	37
4. EXPERIMENTAL.....	38
4.1. Material	38
4.2. Specimen preparation.....	41
4.2.1 Matrix solution.....	41
4.2.2 Dye mixing	41
4.2.3 Casting thin film.....	44
4.3 Color converter thin film optical properties measurement	44
4.3.1 UV absorption measurement	45

4.3.2 PL quantum efficiency measurement.....	45
5. RESULTS AND DISCUSSION	47
5.1 Optical properties of the Coumarion 334 host dye	47
5.1.1 Absorption.....	47
5.1.2 Photoluminance (PL) quantum efficiency	53
5.2 Two-dye system (Coumarin 334 and Pyrromethene 580 in PMMA).....	53
5.2.1 Concentration influence of the dye-pair on the PL quantum efficiency.....	60
5.2.2 Data analysis with energy transfer model.....	65
5.2.3 Color purity of C334 with Py580 two-dye system.....	73
5.2.4 The stability of C334 with Py580 two-dye system.....	76
6. CONCLUSIONS	79
REFERENCES	80

LIST OF FIGURES

	Page
Fig.1 Schematic cross section of typical multilayer organic light-emitting Devices	4
Fig.2 Band structure diagram for multilayer organic light-emitting devices	5
Fig.3 Schematic cross section of single layer organic light-emitting devices	7
Fig.4 Architectures for implementing full-color pixels with OLED	10
Fig.5 CIE diagram	14
Fig.6 The structure of common laser dyes	17
Fig.7 Plot of dye doping level versus OLED EL quantum efficiency	20
Fig.8 Schematic representation of Forster energy transfer and Dexter transfer	23
Fig.9 The absorption and PL spectrum characteristics of a pair matched dye	26
Fig.10 Diagram illustrating the three configurations of the specimen Required for the PL quantum efficiency measurement	28
Fig.11 The complete spectra for the measurement of a thin film MEH-PPV	30
Fig.12 The basic setup for the modified PL quantum efficiency	31

	Page
Fig.13	Diagram illustrating the three steps for the modified PL quantum efficiency measurement 33
Fig.14	Expected PL spectra for step2 and step3 36
Fig.15	The structures of coumarin 334 and pyrromethene 580 39
Fig.16	PL spectrum of 13% C334 in DCE and UV absorption Spectrum of 5% Py580 in DCE 40
Fig.17	UV absorption spectra for various concentration of C334 in PMMA matrix 50
Fig.18	Shift of the maximum absorption wavelength with C334 concentration 51
Fig.19	Optical density vs. C334 concentration for C334 in PMMA matrix one-dye system 52
Fig.20	PL spectra for different concentration C334 in PMMA Matrix one-dye system 54
Fig.21	Concentration influence on the quantum efficiency for C334 one-dye system 55
Fig.22	Concentration effect of Py580 on PL quantum efficiency for Py580 in PMMA matrix one-dye system 56

	Page
Fig.23 Drift of the PL wavelength maximum as a function of C334 concentration	57
Fig.24 Brightness for C334 one-dye system as a function C334 concentration	58
Fig.25 PL spectra of 3.99% C334 in PMMA matrix and 3.99% C334 with 0.036% Py580 in PMMA matrix	59
Fig.26 Dye pair concentration influence on the PL quantum Efficiency for C334 + Py580 two-dye system	64
Fig.27 PL quantum efficiency dependency on various concentration Of C334(host dye) with fixed concentration (0.1%) of Py580	66
Fig.28 The brightness of various concentration of C334 with 0.1% Py580 in PMMA	67
Fig.29 One-dye system energy release model	68
Fig.30 Two-dye system energy transfer and release model	71
Fig.31 Illustration of the definition of η	72
Fig.32 Energy flow for 2% C334 with Py580 in PMMA matrix	74
Fig.33 Energy flow for 4% C334 with Py580 in PMMA matrix	75

Fig.34	PL quantum efficiency decay for the C334/Py580 two-dye system	Page 77
---------------	--	--------------------------

LIST OF TABLES

Table	Page
1. Name and emitted light color of some light-emitting polymers	8
2. The optical properties of some laser dyes	19
3. The experiment procedure for PL quantum efficiency measurement	29
4. The optical properties of Coumarin 334 and Pyrromethene 580	42
5. Storage condition for aging experiment	46
6. Concentration effect of C334 on the absorbance for the one-dye system	48
7. Concentration effect of C334 on the quantum efficiency for the one-dye system	49
8. Concentration effect for 2% C334 + Py580 in PMMA matrix	61
9. Concentration effect for 4% C334 + Py580	62
10. Concentration effect for 8% C334 + Py580 in PMMA	63
11. PL quantum efficiency comparison for C334/Py580 two-dye system stored at different conditions	78

1. Thesis Objective

Research at IBM Almaden Research Center is aimed at optimizing the efficiencies and stability of materials and devices suitable for use in full color OLED (organic light emitting diodes) display applications. The current emphasis is on the selection of dye materials for patterned color converters that may absorb the blue light from the organic diodes and re-emit red or green light appropriately. As a joint study between IBM and SJSU, the main focus of the thesis project is measurement of the quantum efficiency of photoluminescence of a two-dye system in color conversion to green light. Additionally, the decay of quantum efficiency of the two-dye color converter in air and exposed to fluorescent light will be scoped.

Specifically, the thesis will focus on the following:

- (1) Develop a measurement method of dye quantum efficiency for color conversion polymeric thin films
- (2) Investigate the concentration effect of the dye on UV absorption and PL quantum efficiency for the color converter doped with one dye
- (3) Investigate the relationship between the dye pair concentrations and the quantum efficiency for the converter thin film doped with two dyes.
- (4) Investigate the environment decay of the PL quantum efficiency for the two-dye system.

2. Introduction

Today, displays are found in thousands of products from wristwatches and cellular telephones to notebook computers and TVs; they are also the key component in the plethora of emerging communications and computing products. To meet the increasingly complex demands of these Information Age products, the display industry is currently focusing on the development of new light-emitting device technologies for flat panel display. The primary motivation is to replace the bulky and energy consuming traditional TV screen--- cathode ray tubes (CRT)--- with energy efficient flat panels. Liquid crystal displays (LCD) are a reasonable substitute for CRT, and currently dominate the flat panel display industry. LCD operate on the principle that liquid crystalline molecules are mechanically oriented by an external electric field, and therefore a thin film becomes opaque with a polarized back light¹. Although LCD offers high resolution and low power consumption, their application in flat panel display is accompanied by several disadvantages, such as the low response speed, requirement for backlight, and restricted viewing angle. As an emissive technology, organic light emitting diodes (OLED) have attracted much attention for the past decade and have become the leading candidate challenging LCD as the technology-of-choice for the next generation of flat panel display technology because of their better performance. Compared with LCD, OLED offer lighter weight, higher brightness, lower power consumption, and a wider viewing angle^{2,3}. Even more, OLED may be made sufficiently thin to be flexible and convenient. These

These promising properties make them attractive for a multitude of applications. The potential applications include multi/full color cellular phone displays, head mounted displays, full color high-resolution personal digital assistants, heads-up instrumentation for cars, automobile light systems, ultra-lightweight wall-size high definition televisions and even electronic roll-up daily-refreshable newspaper, etc ⁴.

3. Background and Principles

3.1 Basic Structure of an organic light emitting diode device

The basic structure of an organic light emitting diode device is simple: several organic layers are sandwiched between two electrodes (anode and cathode), one of which is transparent. Those organic layers include a hole injection/transport layer adjacent to the anode and an electron injection/transport layer adjacent to the cathode, with the emitting layer (EL) occurring in the middle of the sandwich as shown in Fig1.

Under a dc bias of 2 to 20 volts, electrons are injected from a low work function ($\Phi_w \sim 3$ to 4eV) cathode, and holes are injected from a high work function ($\Phi_w \sim 5\text{eV}$) anode into the electron transporting layer and hole transporting layer, respectively. The electrons and holes travel in the applied field until they meet at the emitting layer, where they combine and form a luminescent excited state; i.e. light shines. The typical band structure diagram for the multilayer device is shown in Fig 2 ⁵.

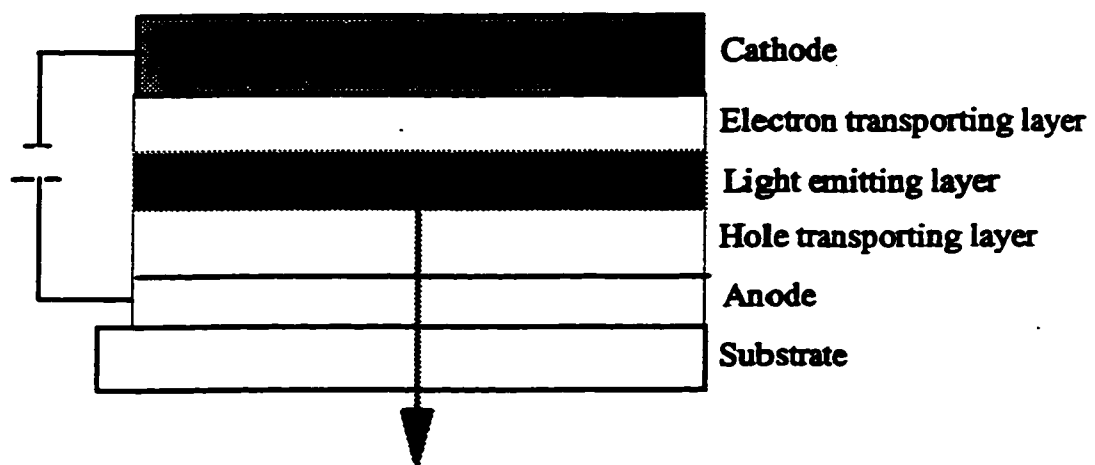


Fig.1 Schematic cross section of multilayer OLED

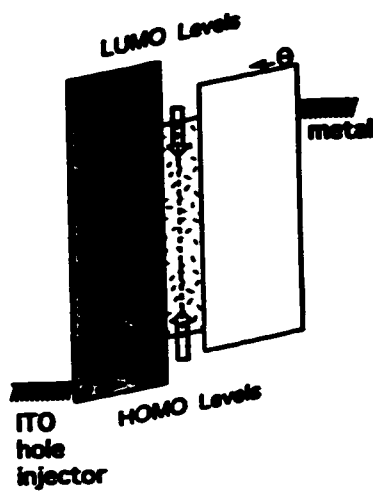


Fig.2 Band Structure diagram for a multilayer organic light-emitting device (OLED)

Source: G. Gu and Stephen R. Forrest, "Design of Flat-Panel Display Based on Organic Light-Emitting Devices," IEEE Journal of Selected Topics in Quantum Electronic, Vol.4, No.1(1998):83

Sometime the organic material of the emitting layer can perform two or even all three functions: hole transport, electron transport, and emission. Therefore the device can be simplified as a double or a single layer device: anode/organic/cathode (Fig3) ⁵.

3.2 Progress in OLED development

The progress in OLED materials and devices since their discovery in 1965 by Helfrich and Schneider⁶ has been impressive. Threshold voltages for light emitting have fallen from several thousand volts to just 2 to 3 V for today's light emitting polymers. The efficient conversion of electrical power to front-of-screen luminance has achieved 30 lm/w and brightness (luminance) in excess of 100 cd/m² (commonly 70 cd/m² for today's battery-operated LCD notebook) are readily available. The operating lifetime of the light-emitting material is over 10,000 hours. A wide range of materials has been reported that efficiently produces emitting light throughout the visible spectrum ⁷. Table 1 shows the chemical names and the emitted light colors of some examples of light emitting polymers ⁸.

Although dramatic improvements have been made in OLED technology, there are still many hurdles to overcome before they can compete with LCD. One of them is to find an inexpensive method to manufacture a full color display.

3.3 Red, green and blue (RGB) form for creating full color

The RGB form is the method of creating color by mixing various proportions of three distinct stimuli colors: red, green and blue ⁹. From far, unable to distinguish

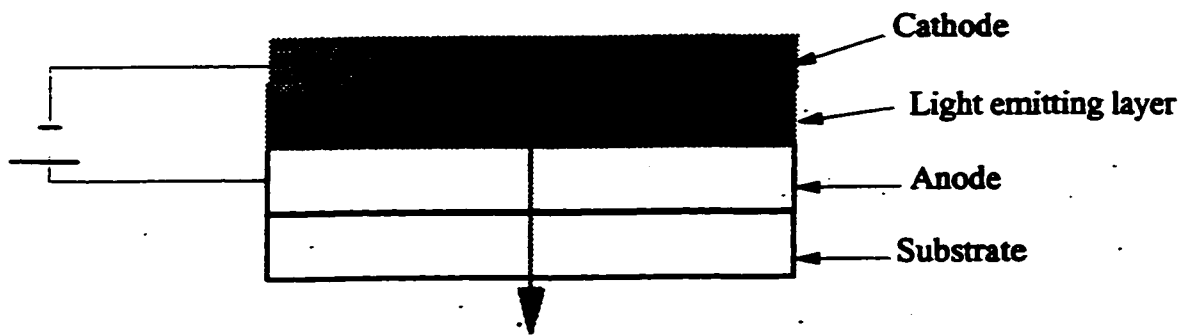


Fig.3 Schematic cross section of a single layer organic light-emitting device

Table 1. Name and emitted light color of some light-emitting polymers
Source: J. Campbell Scott and George G. Malliaras, "The Chemistry, physics and engineering of organic light-emitting diodes", Wiley-VCH, Weinheim, 1999 (in press)

Name	Color of emitted light
Poly(phenylenevinylene) (PPV)	Yellow-green
Poly[2-methoxy-5-2'-ethyl-hexoxy-1,4-phenylene vinylene] (MEH-PPV)	Orange-red
Laddered poly-paraphenylene (LPPP)	Blue

individual color dots, these colors are merged by the human brain and are seen as combined colors.

For example:

1 Red + 1 Green = Yellow

1 Red + 1 Blue = Magenta

So by creating the three primary colors, we can obtain full color.

3.4 Suggested color tuning technology for OLEDs

Several potential strategies have been suggested¹⁰ for color tuning in OLED, as illustrated schematically in Fig.4⁸. Each of the architectures will next be described.

3.4.1 Patterned emitters.

The conceptually simple approach to full-color is to directly pattern red, green and blue EL pixels side by side in a patterned array. Since this technique requires a different organic thin film for each OLED, it is useful only at low resolution because of the limitation of patterned feature size.

3.4.2. Microcavities.

The filtering effects of various microcavity structures have been used to influence the directionality and color of OLED. This approach is complicated in terms of patterning and fabrication because both the organic stack and the bottom electrode must be patterned with three different microcavity thicknesses for red, green or blue.

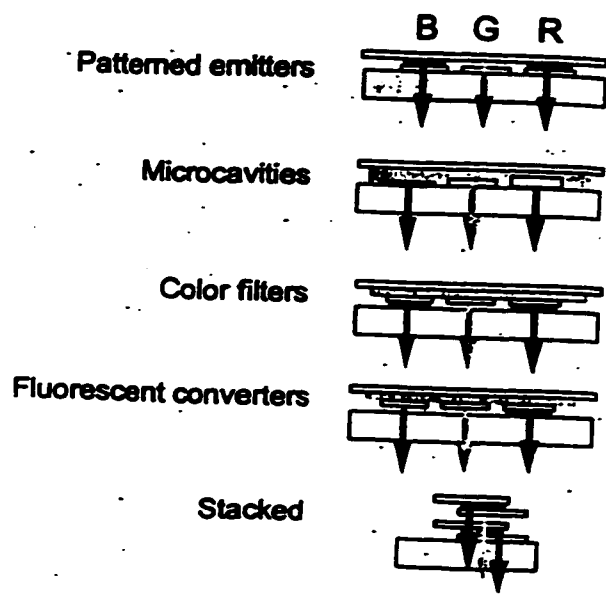


Fig.4 Architectures for implementing full-color pixels with OLED

Source: J.C. Scott and G.G. Malliaras, " The Chemistry, physics and engineering of organic light-emitting diodes", Wiley-VCH, Weinheim, 1999 (in press)

3.4.3. Color filters.

In this technology, the OLED is made to emit white light and separately patterned to filter red, green and blue. The drawback of this technique is that at least 2/3 of the emitted light is absorbed in the primary colors filters with a subsequent loss in overall power efficiency.

3.4.4. Stacked OLED

At least three sub-pixels, which emit red, green or blue light respectively, are stacked one on top of the other to make a single full-color element. Obviously this technique requires that the two electrodes in the middle of the structure must be transparent. This allows the entire areas of stacked pixels to emit and mix primary stacked colors, which provides for a full color display.

3.4.5. Fluorescent converters.

In this method, a blue light-emitting layer is used as the emitter. Fluorescent converters--- dye-doped polymer thin films, are patterned underneath to produce the desired color (red or green). Because each converter consists of fluorescent material (the dye), it can efficiently absorb blue light and re-emit either green or red light. In principle, this technique can overcome much of the power loss associated with color filters.

3.5 The criterion for a good dye in a fluorescent converter system

Typically a good dye should meet the following criteria to exhibit satisfied output for a color converter: (a) high color purity; (b) high absorption of the incident light; (c) high quantum efficiency of photoluminescence. Each of these will be discussed next.

3.5.1. High purity of the desired color

When dealing with color, it is important to have quantitative means to evaluate the color and its saturation (purity). The common used system is the CIE system (CIE: Commission Internationale de l'Eclairage). CIE is an international standard and is based on the fact that any pure (monochromatic) color can be visually matched by an additive mixture of red, green, and blue light in the appropriate proportions. That is

$$X \text{ Red} + Y \text{ Green} + Z \text{ Blue} = \text{Perceived color} \quad (\text{Eq.1})$$

In color matching experiments, any color with a given emission wavelength has a given (X, Y, Z) number. Based on the tristimulus response of a standard observers' (r_λ , g_λ , b_λ), the (X, Y, Z) number can be calculated from the light PL spectrum using the following formulas:

$$X = \int P_\lambda r_\lambda d\lambda \quad (\text{Eq.2})$$

$$Y = \int P_\lambda g_\lambda d\lambda \quad (\text{Eq.3})$$

$$Z = \int P_\lambda b_\lambda d\lambda \quad (\text{Eq.4})$$

Where, P_λ is the intensity of certain wavelength in the PL spectrum.

In order to represent these values on a two dimensional plot, X, Y, and Z are converted to their fractional contributions as:

$$x = \frac{X}{X+Y+Z} \quad (\text{Eq.5})$$

$$y = \frac{Y}{X+Y+Z} \quad (\text{Eq.6})$$

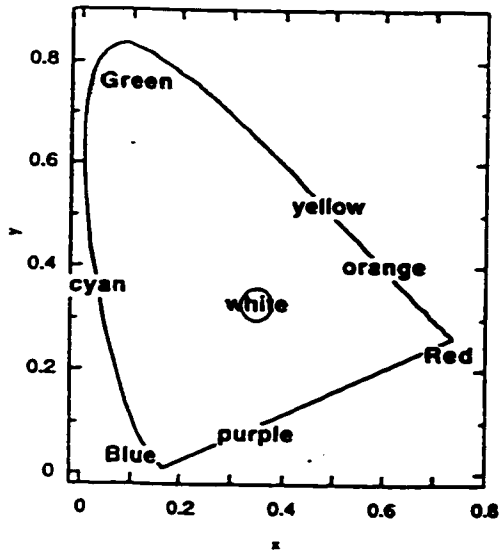
$$z = \frac{Z}{X+Y+Z} \quad (\text{Eq.7})$$

The plot of x vs. y for all visible colors is called the CIE diagram. (See Fig 5)

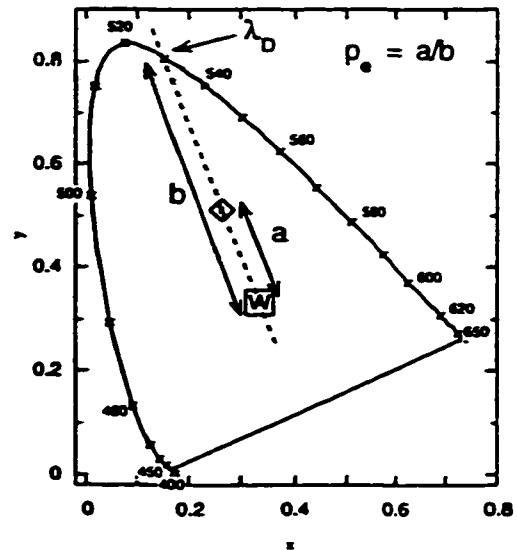
In the CIE diagram, monochromatic colors fall on the edge of the horseshoe shaped curve. White is located at the center of the CIE diagram (Fig.5(a)). When a given point (x, y) is moved towards the center from the edge, the chrominance remains the same but the color becomes progressively more unsaturated (i.e., the hue changes). The wavelength, λ_D , of a color represented by an (x, y) coordinate inside the CIE curve is defined by the projected intersection of a straight line connecting the central white point and the (x, y) point with the CIE bounding curve (see Fig.5 (b)). The purity of the color, P_e , is defined as the ratio $\frac{a}{b}$ (see definition in Fig.5 (b)). Pixels of high P_e values are very important in full color display application.

3.5.2 High absorption of the incident light

In the fluorescent converter, high absorption of the incident light is one of the important issues.



(a) CIE diagram



(b) Definition of purity

Fig.5 CIE diagram

Source: G. Gu and Stephen R. Forrest, "Design of Flat-Panel Display Based on Organic Light-Emitting Devices," IEEE Journal of Selected Topics in Quantum Electronic, Vol.4, No.1(1998):83

According to the Beer-Lambert Law, when a parallel beam of light of intensity (I_0) is directed on a low concentration solution, C , the relationship between the intensity of the transmission (I) and incident light intensity (I_0) can be represented by (Eq.8).

$$\text{Log}_{10} (I_0/I) = \epsilon CL \quad (\text{Eq.8})$$

where $\text{Log}_{10}(I_0/I)$ is known as the optical density (OD) or absorbance of the solution, C is the concentration measured in moles per liter, L is the transmission distance, and ϵ is the molecular extinction coefficient. There will be a linear relationship between the absorbance and solution concentration at fixed transmission distance for a dilute solution. Therefore a higher concentration of the solution in a low concentration range results in higher absorbance¹¹.

3.5.3 High quantum efficiency of photoluminance

The measurement of the absolute fluorescence yield efficiency is very important because only based on its accurate measurement can one chose the right converter materials and optimize the concentration of the selected dye material. In this study, the absolute photoluminescence efficiency, η , is defined by Eq.9¹².

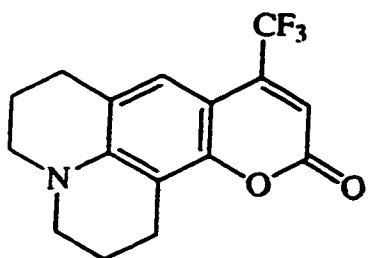
$$\eta = \frac{\textit{number of photons emitted}}{\textit{number of photons absorbed}} \quad (\text{Eq.9})$$

3.6 External color conversion

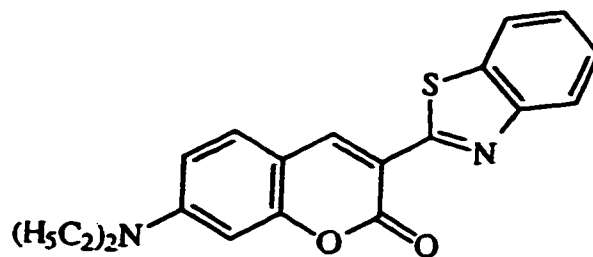
Many groups around the world are investigating color-tuning research. A few researchers refer to internal color conversion (such as adding dye in either the emitting layer, the hole transport layer or the electron transport layer regions). Only Hosokawa *et al*⁷ from Japan reported achievement of multicolor by using color conversion (external conversion), though they did not give details. Whether full color is achieved via external or internal conversion, the common characteristic of the reported color tuning methods is that photoluminescence dye dopants have been successfully incorporated into a variety of OLED structures and materials. Several publications^{5,7,12,13,14} discuss related issues and present important information. They are reviewed in the following discussion.

3.6.1 Doped dye materials

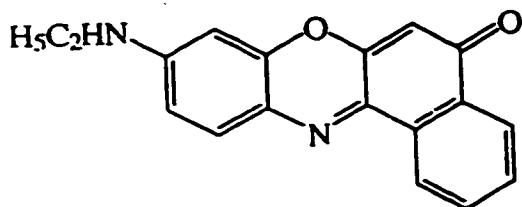
In this project, the color converter is a dye doped thin film and the matrix is PMMA (polymethylmethacrylate, $T_g = 110^\circ\text{C}$, $\rho = 1.188\text{g/cm}^3$). Based on the working function of a color converter, the dye doped in the converter must absorb visible light. In the IBM application, the dye should absorb visible light around 460nm wavelength. Common laser dye material may be employed as the dopant. Examples of these laser dyes are coumarin 153, coumarin 6, phenoxazone 9 (Nile 9) and pyrromethene 650. Their structures are shown in Fig 6. All of these dyes have conjugated structure---that is, they contain alternating single and double carbon bonds in the organic compounds. This structure is called π bonding and allows the electrons to move over longer distance than in the case of



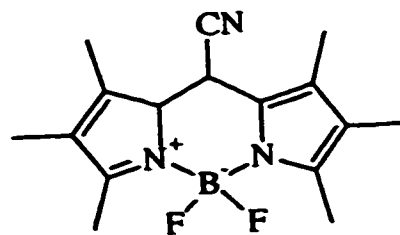
Coumarin 153



Coumarin 6



Phenoxazine 9



Pyrromethene 650

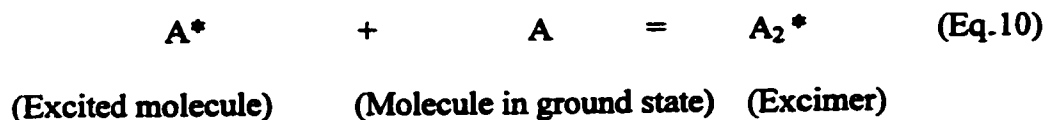
Fig.6 The structure of common laser dyes

a saturated structure. Therefore the energy needed to create an excited state in the π bonding structure is much less than that required of an ordinary single or double bond organic molecules. Hence these materials can absorb wavelengths in the visible light spectrum. Table 2 gives some of the common optical properties of these dyes ¹⁵.

3.6.2. Dye concentration effects

C. Wu, J. C. Strum and R. A. Register *et al*¹³ reported that it is very important to keep the dye dopant in low concentration for OLED electroluminescence (EL) quantum efficiency, because the increase of the concentration of the fluorescence solute commonly causes a decrease in the molecular fluorescence quantum yield¹⁴. The relationship between external EL quantum efficiency and dye loading level is show in Fig.7.

Fig.7 shows that the EL quantum efficiency drops rapidly when the dye concentration exceeds 1%. Concentration quenching (also called self-quenching) causes this luminescence loss. At high concentration, the dye molecules begin to aggregate and the separation distance between them decreases. It becomes easy for the excited dye molecule to interact with a nearby unexcited dye molecule and form an excited dimer, which is called an excimer. The applicable reaction is:



Although an excimer can exhibit luminescence, it does so with low quantum efficiency. In addition to the low quantum efficiency, Birks indicated in his book

Table 2. The optical properties of some laser dyes

Source: A. Luque, and E. Lorenzo, " Conditions for Achieving Ideal and Lambertian Symmetrical Solar Concentrations," Applied Optics Vol.20, No.21(1982): 3736.

Dye	Chemical name	Molecular weight	Absorption max (nm)	Emission max (nm)	Color
Coumarin 153	3H,6H,10H-Tetrahydro-8-trifluoromethyl[1]benzopyrano-(9,9a,1-gh)quinolizin-10-one	309.29	423 in EtOH	530	green
Coumarin 6	3-(2'-Benzothiazolyl)-7-diethylaminocoumarin	350.44	458	505	green
Pyromethene 650	4,4-difluoro-8-cyanon-1,2,3,5,6,7-hexamethyl-4-bora-3a,4a-diaza-s-indacene	303.16	590	612	red
Phenoxazine 9	9-diethylamino-5H-benzo(a)phenoxazin-5-one	318.37	550	636	red

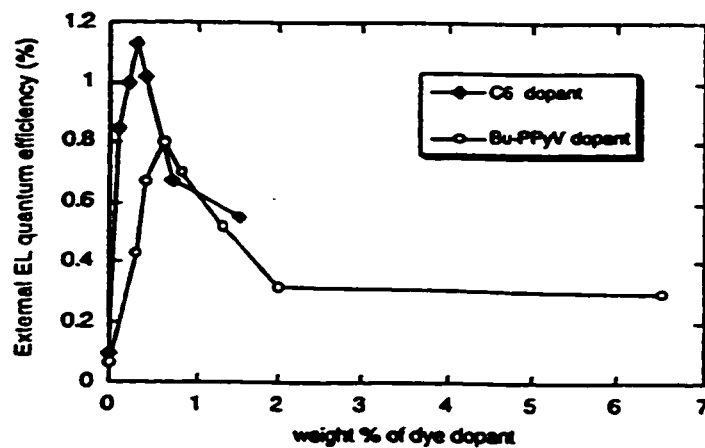


Fig.7 Plot of dye doping level versus OLED EL quantum efficiency
Source: G. Gu and Stephen R. Forrest, "Design of Flat-Panel Display Based on Organic Light-Emitting Devices," IEEE Journal of Selected Topics in Quantum Electronic, Vol.4, No.1(1998):83

“Photophysics of Aromatic Molecules” that another disadvantage of high level loading is the broadness of the emission band ^{5,14}.

3.6.3 Energy transfer involved in the dye photoluminance (PL) process.

After a dye molecule absorbs energy at some wavelength, it becomes an excited molecule. It is possible that the excited molecule will not return to the ground state by emission of a photon immediately, but rather energy may be transferred to another dye molecule. We define the excited molecule as the donor and a second dye molecule at its ground state as the acceptor. There is energy transfer involved in dye PL process in thin films as is shown by Shoustikov, You and Thompson⁵. In their paper, two energy transfer mechanisms are reviewed: (a) Forster energy transfer, and (b) Dexter energy transfer. A schematic representation of each energy transfer process is illustrated in Figure 8 and is further explained below.

3.6.3.1 Forster energy transfer mechanism

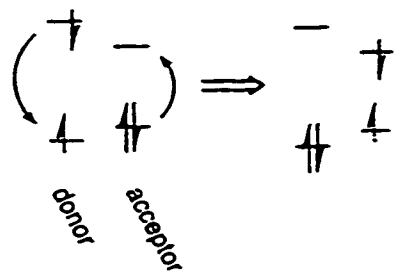
Forster energy transfer involves a dipole-dipole coupling of the transition dipole moments. As the excited donor relaxes, its energy is transferred via a strong Coulomb interaction to a neighbor dye molecule. This interaction can transfer over long distance (up to 100Å) and this distance is called the Forster radius. There exists a characteristic Forster radius R_0 in every specific dye system. Forster energy transfer has a high probability of occurrence if the donor-acceptor separation is within R_0 . The typical radius

for Forster energy transfer is 30 –200Å. The larger the Forster radius, the quicker the energy transfer process⁵. R_0 is proportional to the degree of spectral overlap between the donor PL and acceptor absorption spectra⁵. The high rate of the Forster energy transfer is favored at a high degree of overlap.

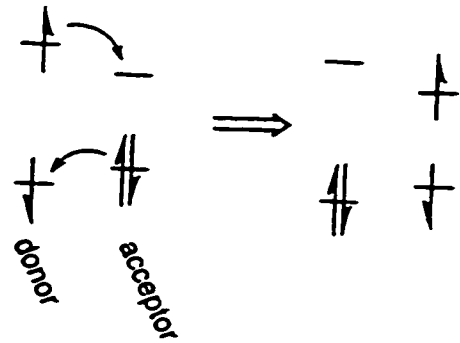
3.6.3.2 Dexter mechanism energy transfer mechanism

The Dexter mechanism achieves energy transfer via electron exchange. The rate of Dexter energy transfer decreases rapidly as the donor-acceptor separation distance increases. The typical radius for Dexter energy transfer is below 20Å. The rate of Dexter energy transfer is also favored by a large overlap between the donor emission and the acceptor absorption⁵.

Both of the Forster mechanism and Dexter mechanism are alternative energy transfer processes. At large separation distance, i.e. low dye concentration, which is desired for OLED color conversion, the Forster mechanism may dominate the energy transfer process since the Dexter mechanism will require electron transfer. To decrease the energy transfer loss, the overlap of the acceptor absorption and the donor photoluminance must be evaluated. In this way, one can choose the potential dye candidates for color converter applications.



Forster energy transfer



Dexter energy transfer

Fig.8 Schematic representation of Förster energy transfer and Dexter transfer

Source: G. Gu and Stephen R. Forrest, "Design of Flat-Panel Display Based on Organic Light-Emitting Devices," *IEEE Journal of Selected Topics in Quantum Electronic*, Vol.4, No.1(1998):83

3.6.4. A two-dye photoluminescence approach

C. A. Parker¹¹ cites that the intensity of fluorescence emission, Q , is equal to the intensity of absorption multiplied by the quantum efficiency.

$$Q = A \times \eta \quad (\text{Eq.11})$$

That is, the brightness of the converter is directly proportional to both absorbance and quantum efficiency of the fluorescence process.

From the theory of absorption and the work of Wu *et al*¹³, we know that the absorption of light is proportional to the concentration of the dye (See the Beer's Law, Eq.2). The higher the dye concentration, the greater the absorption. On the other hand, the quantum efficiency, η , follows an opposite trend. Too high a dye concentration results in very low quantum efficiency. It thus can be concluded that one cannot expect a converter doped with one dye to give high brightness even if the concentration were to be optimized. Two dyes are required to obtain the high absorption and high quantum efficiency concurrently. The hypothesis is cited next.

To meet the absorbance and quantum efficiency requirement for color converter applications, a two-dye system approach for the converter thin film is taken. Two dyes are used to dope in the converter thin film. One dye (called the host dye) is present at a relatively high concentration (2 wt % to 10 wt %). The role of the host dye is to absorb the incident blue light. The second dye (called the guest dye) at relatively low concentration (0.1wt% to 1 wt%) will convert the available excitation energy to primary color re-emission. Molecular energy transfer is the means by which the absorbed energy can be passed by the host dye to the guest dye (section 3.6.4). The energy is released by

the guest for an optical fluorescence. To optimize the converter, the host is expected to exhibit high absorption ($OD > 1/\mu\text{m}$) and the guest must have high quantum efficiency. The combination will yield high brightness. Since absorption increases with increased host dye concentration and quantum efficiency increases with decreased guest concentration, there will be a peak in efficiency of the two-dye system as function of the dye-pair concentration. The goals of this research are to develop a reproducible and accurate method to determine quantum efficiency of color converter thin film; and to evaluate the quantum efficiency of a two-dye system (C334 and Py580) quantitatively.

3.6.4.1. The criterion for choosing two-dye candidates

In a two-dye system for fluorescent converter application for OLEDs, one dye must exhibit efficient absorption around 460nm and the second dye must exhibit a PL peak near the desired wavelength (for example, for green color, the PL emission should be at 520nm). In addition, the two dyes must have a large overlap between the host emission and the guest absorption, because based on the Forster transfer mechanism, the rate of energy transfer is favored for large overlap, which leads to quick energy transfer from the host dye to the guest dye. The schematic absorption and emission spectra are illuminated in Fig.9.

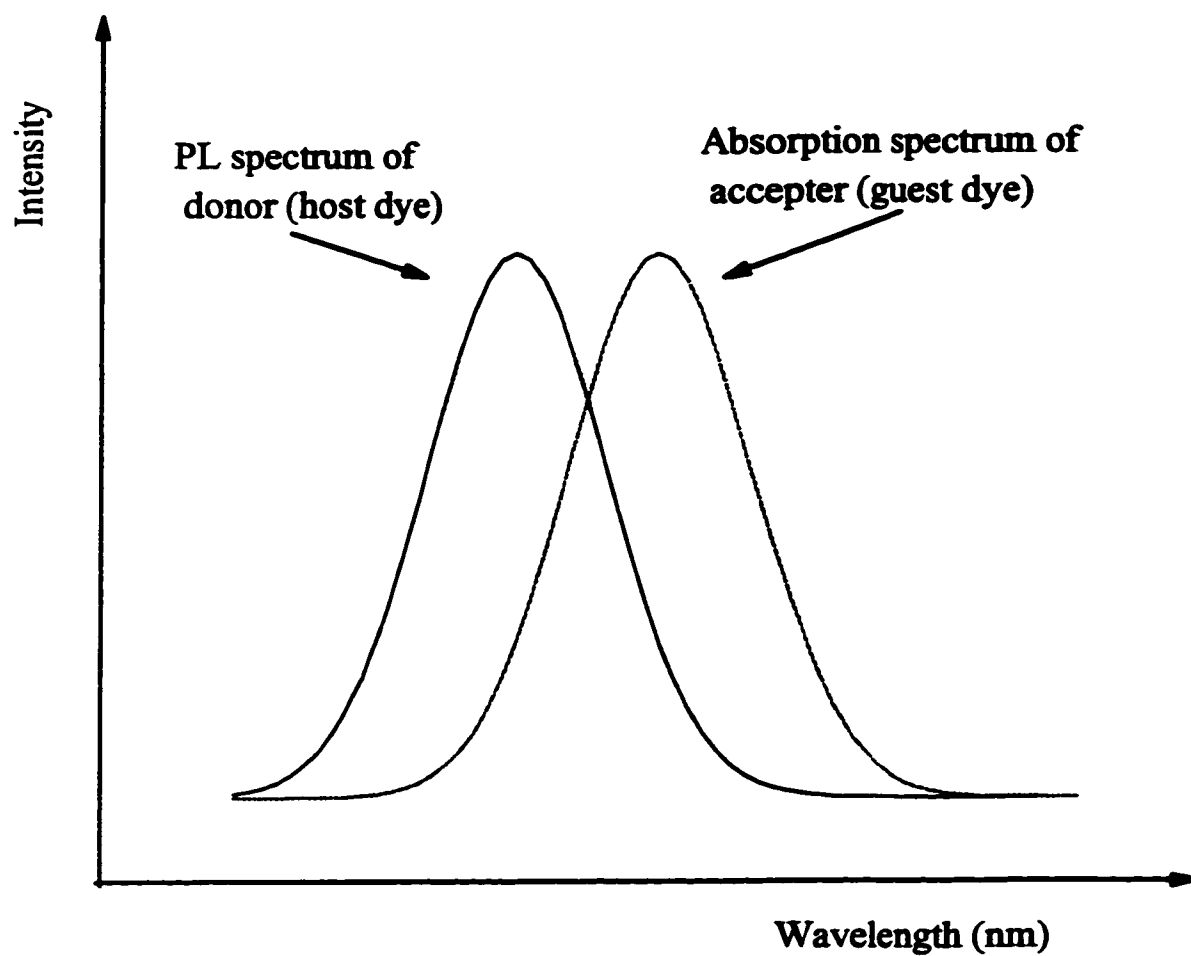


Fig.9 The absorption and PL spectrum characteristics of a pair matched dye

3.7. A measurement method for the quantum efficiency

J.C. de Mello, H.F. Wittmann, and R.H. Friend¹² report an improved experimental method to determine the photoluminescence quantum efficiency of thin film specimens. The key element of this method is incorporation of an *integrating sphere* in the measurement method. An integrating sphere is a hollow sphere with an inner surface coated with a diffusely reflecting white material (BaSO₄). When a light is placed in an ideal integrating sphere, the light is redistributed isotropically over the interior surface of the sphere. This eliminates the angular dependence of the emission. The experimental setup and three steps essential to determine PL efficiency will next be explained using the illustrating of Fig.10. Each step of Fig.10 is defined in Table 3.

A CCD Spectrometer is used to detect the spectrum. The experiment procedure and respective relations are shown in Table.3. The complete spectra for measurement of a MEH-PPV(PPV doped with the dye MEH) thin film specimen is shown in Fig.11.

In the intensity vs. wavelength PL spectra, the integrated area of each peak is proportional to the amount of energy of the optical spectra (i.e. energy of a particular color band is equal to area under the respective color peak). The area under the source laser profile is defined as L; the area under the re-emitted profile is defined as P; The fraction of the scattering light absorbed by specimen in experiment (b) is μ ; the fraction of the incident light absorbed by the specimen is A; and the quantum efficiency is η . Next, consider how the values of absorption (A) and quantum efficiency, η , are determined from the series of experiments illustrated in Fig.12 and defined in Table 3.

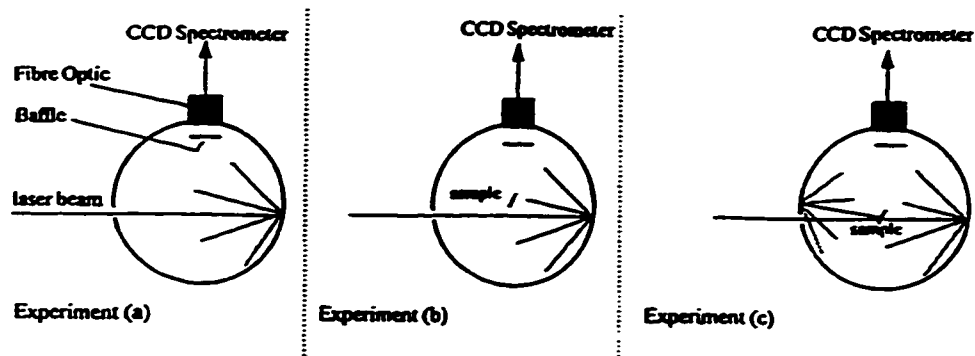


Fig.10 Diagram illustrating the three configurations of the specimen required for the PL quantum efficiency measurement

Source: J. C. de Mello, H. F. Wittmann, and R. H. Friend, " An Improved Experimental Determination of External Photoluminescence Quantum Efficiency," Advanced Materials, No.3(1997): 231

Table 3. The experiment procedure for PL quantum efficiency measurement

*Source: John C. de Mello, H. Felix Wittmann, and Richard H. Friend,
 " An Improved Experiment Determination of External Photoluminescence
 Quantum Efficiency," Advanced Materials, Vol.9, No.3 (1997):230-232*

Step	Operation	Respective relations	Equation number
1 Experiment (a) in Fig.5	The sphere is empty. Measure L_a . Incident light hit the sphere wall and reflects and scatters. Collect spectra.	L_a is the area under source laser peak	
2 Experiment (b) in Fig.5	Specimen placed in sphere but laser not incident on specimen directly. The specimen absorbs the scattered light and emits. Collect spectra. The detected signal is composed of scattered laser light and the fluorescence light.	$L_b = L_a \times (1 - \mu)$ Goal: obtain μ	I
3 (Experiment (c) in Fig5)	Laser beam is directed onto the specimen. Collect spectra.	$L_c = L_a \times (1 - A) \times (1 - \mu)$ Goal: obtain A $L_c + P_c = (1 - A) \times L_b + P_b + \eta L_a A$ Goal: obtain η	II III

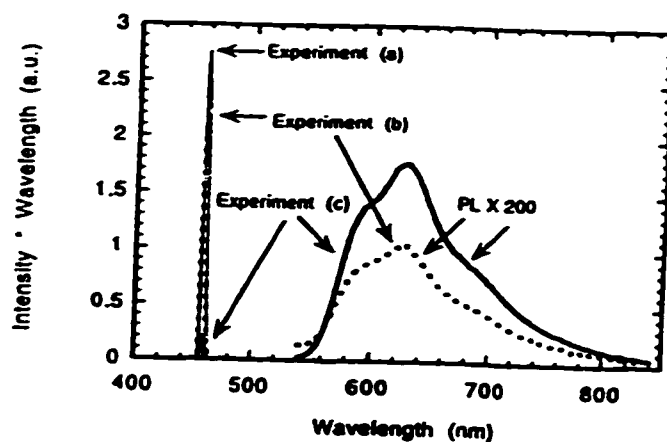


Fig.11 The complete spectra for the measurement of a thin film MEH-PPV

Source: J.C. de Mello, H. F. Wittmann, R. H. Friend, " An Improved Experimental Determination of External Photoluminescence Quantum Efficiency," Advance Materials, Vol.9, No.3(1997): 231

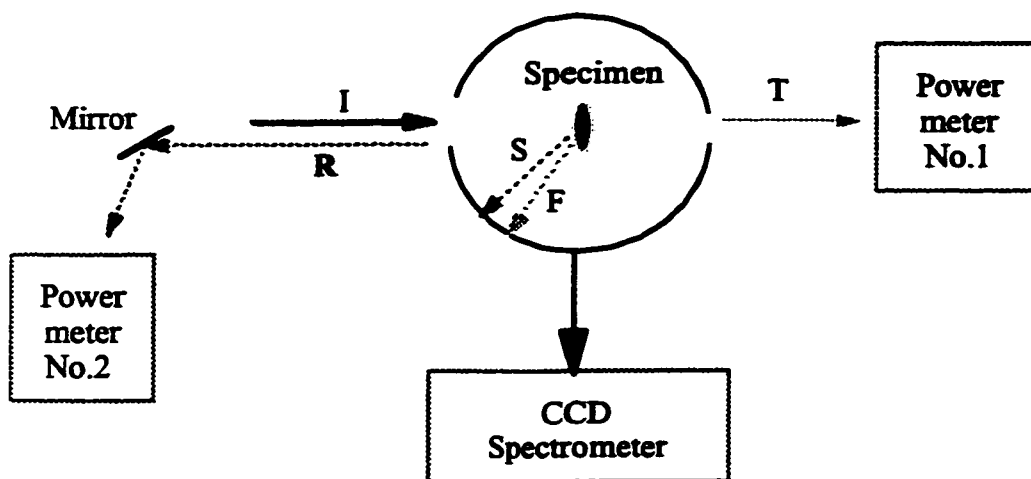


Fig.12 The basic setup for the modified PL quantum efficiency

From Eq.I and Eq.II in Table 3, we obtain Eq.12:

$$A = (1 - L_c/L_b) \quad (\text{Eq.12})$$

Inserting Eq.12 into Eq.III of Table 3, the quantum efficiency, η , becomes:

$$\eta = \frac{P_c - (1 - A)P_b}{L_a A} \quad (\text{Eq.13})$$

The shortcoming of the deMello method is that the contribution of scattered light to the determination of absorption, μ , is overlooked. Obviously this will effect the measurement accuracy. This concern will next be addressed.

3.8 PL quantum efficiency measurement of this investigation

Fig.12 shows the basic setup for the PL quantum efficiency measurement in this investigation. An integrating sphere is employed in the experiment. Since the integrating sphere has its inner surface coated with diffusely reflecting material, we assume that the intensities of the redistributed light are the same regardless of the redistribution angle. A stimulated laser with a wavelength around 460nm is used as the incident light. A photoluminance spectrometer with a CCD and two power meters are used as detectors. The converter thin film specimen is placed in the sphere and its position can be changed by rotation, either to intercept or to be removed from the path of incident laser light. A sequence of independent measurements is performed by placing the thin-film specimen in three different orientations as shown in Fig.13.

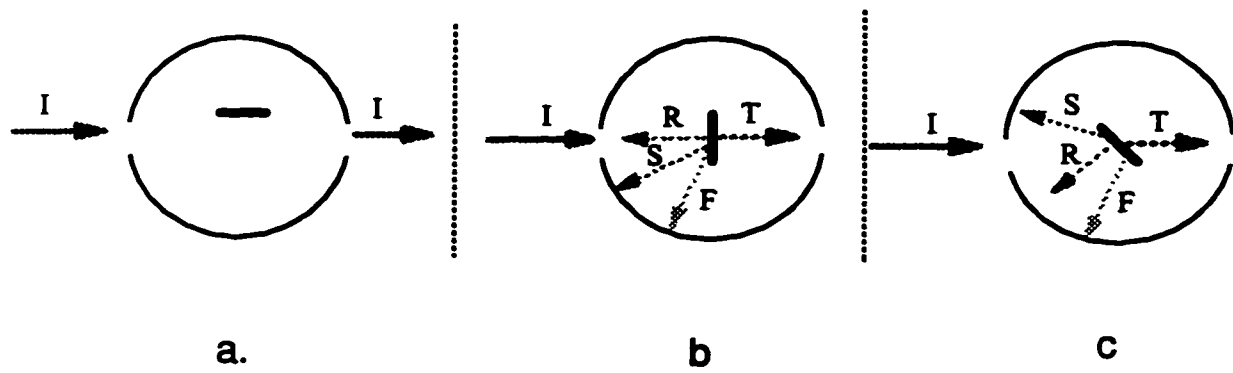


Fig.13 Diagram illustrating the three steps for the modified PL quantum efficiency measurement

With the laser light directed on the specimen, the sum of the energy power of the transmission (T), scattering (S), reflection (R), and absorption (A) is equal to the intensity of the incoming light (I).

$$I = T + R + S + A \quad (\text{Eq.14})$$

When the specimen is rotated out of the way so that the laser is directly incident on the power meter, (see Fig.13 (a)), the incident power, I, is obtained (from the power meter No. 1.)

When the specimen is rotated perpendicular to the incident laser (Fig.13 (b)), the transmission power (T) is measured (from the power meter No.1). The reflected power(R) is measured from power meter No.2. At the same time, the PL spectra can be obtained using the CCD spectrometer. An example PL spectrum is shown in Fig.14 (step 2 orientation).

The scattered light is recorded as the area L₂ under the peak at the laser wavelength around 460nm. The fluorescence peak occurs at a longer wavelength. Since the area under each peak is proportional to the amount of energy of the collected light, if the power coefficient is K, the scattering light energy S is equal to

$$S = K \times L_2 \quad (\text{Eq. 15})$$

The fluorescent light energy, F is a function of area P

$$F = K \times P \quad (\text{Eq.16})$$

When the specimen is rotated and placed off normal (Fig.13 c), the PL spectrum also can be obtained from the CCD spectrometer (see Fig.14 step 2 orientation). The peak at the 459nm (stimulated laser wavelength) comes from the both reflecting and

scattering light components. So the relationship between the reflecting and scattering light energy and the profile area L_3 can be presented by Eq.17:

$$S + R = K \times L_3 \quad (\text{Eq.17})$$

Subtraction of Eq.15 from Eq.17 and reorganization gives the relation:

$$K = \frac{R}{L_3 - L_2} \quad (\text{Eq.18})$$

Substituting the value of R (measured when the sample is placed perpendicular to the incident light), the energy coefficient, K, is determined from Eq.18. The further on scattering light energy, S, can be calculated from Eq.15.

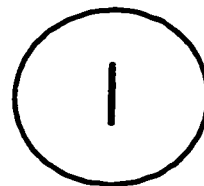
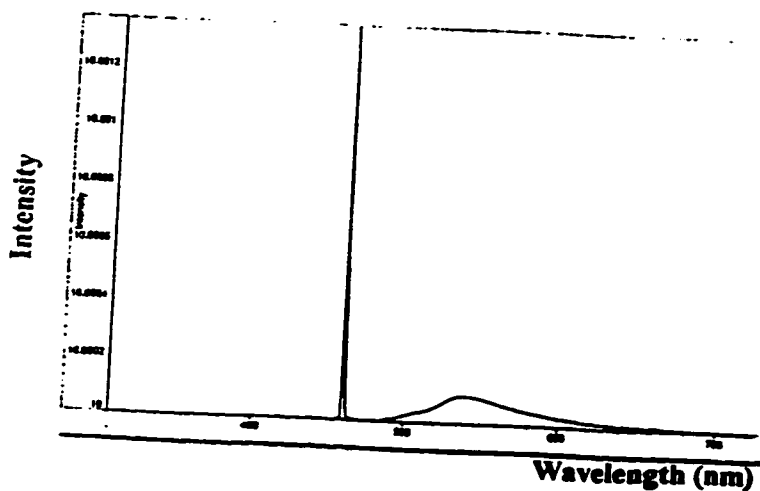
Once the energy of incident light (I), transmission (T), reflection (R), scattering (S), and fluorescence (F) are obtained from the above measurement method, the absorption (A) can easily to be calculated:

$$A = I - T - R - S. \quad (\text{Eq.19})$$

The quantum efficiency is determined from the expression:

$$\eta = \frac{\text{fluorescence}}{\text{Absorption}} = \frac{F}{A} \quad (\text{Eq.20})$$

Step2



Step3

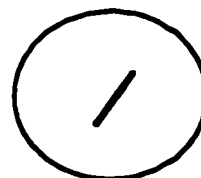
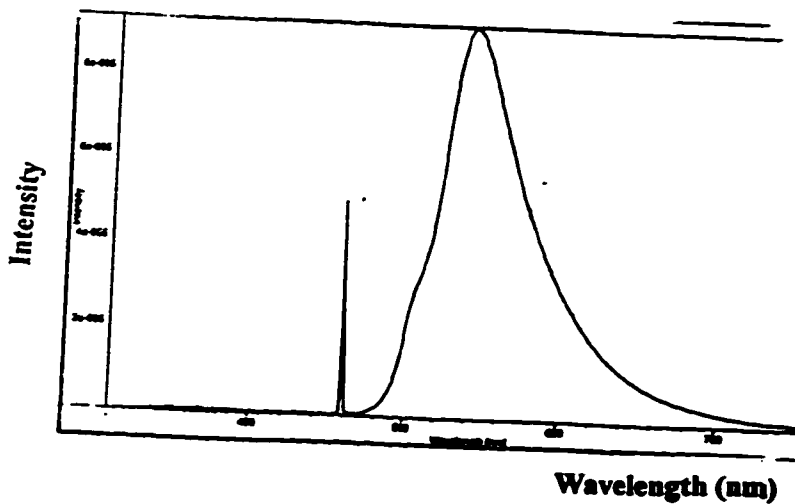


Fig.14 Expected PL spectra for step2 and step3 of Fig.13 (b) and (c) orientation

3.9 Environmental degradation of the color converter thin film

Storage stability of the dyes in the color converter is another important issue of concern. For dye-doped polymer thin films, environmental degradation which leads to the loss of PL quantum efficiency, may happen with exposure to oxygen and/or light. Possible mechanisms for loss of PL quantum efficiency in OLED systems include the followings:

1) Diffusion of impurities (such as O₂, H₂O, etc.)

A dye-doped thin film placed in an oxygen-moisture-containing atmosphere can absorb oxygen (or water). These impurity molecules diffuse into the thin film and create quenching centers which result in decreasing the PL quantum efficiency.

2) Oxidative degradation

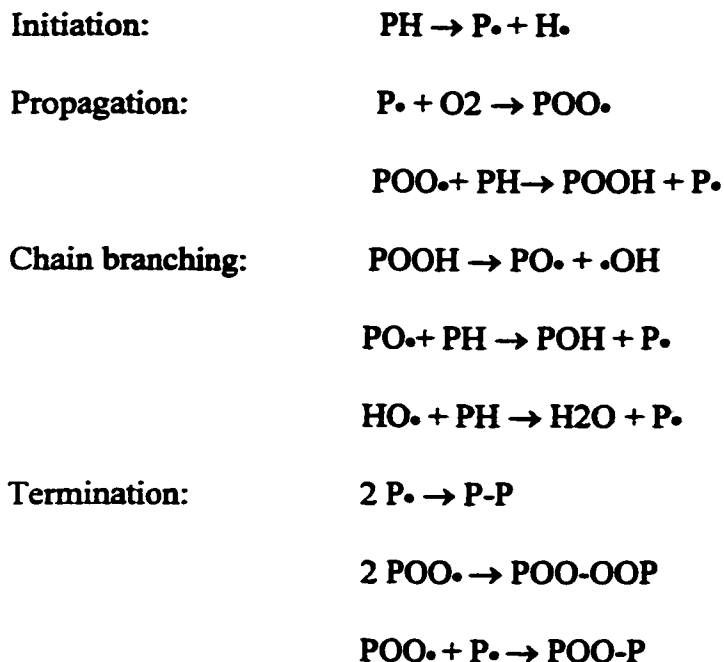
Oxygen molecules diffuse into the thin film and the derivatives of the dye molecule react with O₂, changes the chemical bond states. Quantum efficiency degradation can result.

3) Photodegradation

The dye molecule absorbs radiation light and become energy rich or excited. If the excitation energy reaches the magnitude of the activation energy of bond disruption, the dissociation of some weak bonds may occur and form free radicals. The free radicals rearrange and form an optically inactive product.

4) Photo-oxidation

The photo-oxidation mechanism of many polymers is described by the following sequences¹⁶:

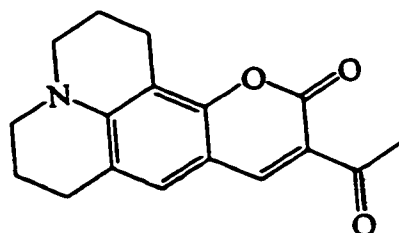


In this manner, some derivatives of the dye molecule can be changed by light/oxygen exposure.

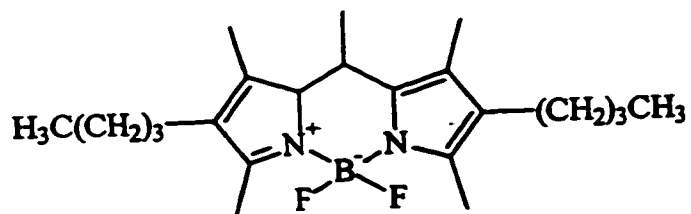
4. Experimental

4.1 Materials

One dye pair ---- coumarin 334 and pyrromethene 580--- is the subject of this thesis. Coumarin 334 was chosen as the host dye and pyrromethene 580 as the guest dye for the color converter because their optical properties meet the overlap requirement of energy transfer (Section 3.6.3). The dye structures are shown in Fig.15 and Fig.16 demonstrates the large emission/absorption overlay.



Coumarin 334



Pyrromethene 580

Fig.15 The structures of coumarin 334 and pyrromethene 580

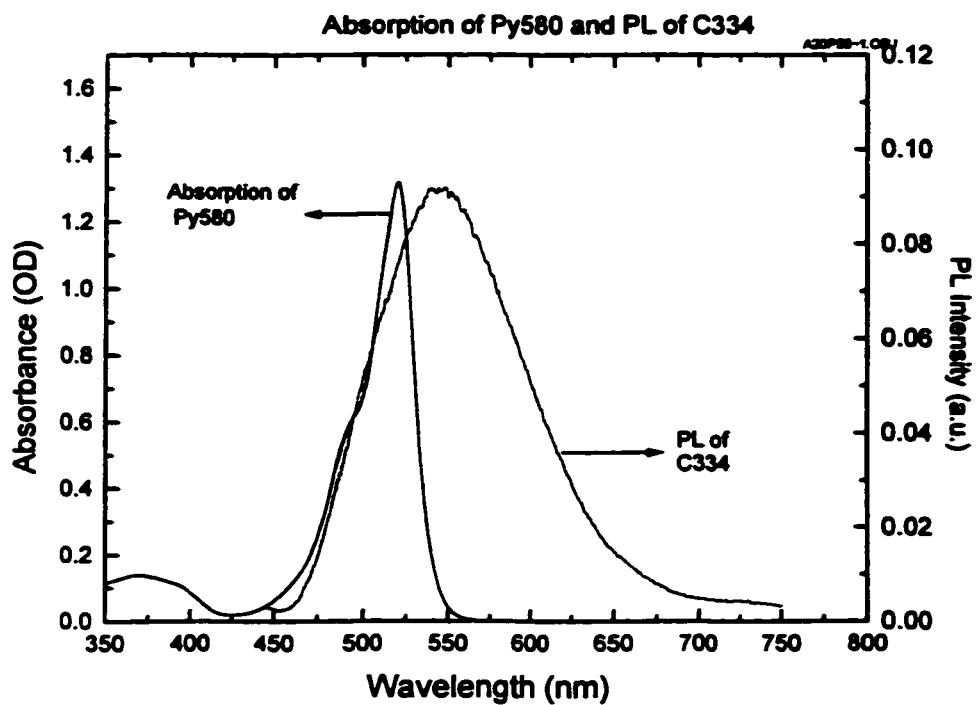


Fig.16 PL spectrum of 13% C334 in DCE and UV absorption spectrum of 5% Py580 in DCE

Source: Previous work of IBM summer students Brian Triplett and Eric Green

Table 4 gives the optical properties of this dye pair. The UV absorption spectrum of pyromethene 580 and photoluminance emission spectra of coumarin 334 are presented in Fig.16. The emission of coumarin 334 and the absorption of pyromethene 580 are shown to have a large overlap, which has the advantage of an efficient rate of energy transfer between the host dye (C334) and the guest dye (Py580). (See section 3.6.3).

The dye pair are doped in a PMMA (Polymethylmethacrylate, $T_g = 110^\circ \text{C}$) matrix and the solvent is DCE (1,2-Dichloroethane).

4.2 Specimen preparation

The specimen preparation consists of four steps: a) make the matrix solution, b) mix the two dyes in the matrix solution, c) spin cast the color converter thin film, d) post bake to cast film. These will be discussed in this section.

4.2.1 Matrix solution

The basic solution for the polymer matrix of the color converter layer is 10 wt% PMMA in DCE. PMMA powder and DCE liquid were mixed to form the solution by tumbling. A minimum of 4 hours tumbling at room temperature is required prior to use.

4.2.2 Dye mixing

A specific weight fraction of C334 (or/and Py580) powder was mixed in 10% PMMA/DCE solution to make the target concentration solution for casting. All concentrations reported here are the weight percent of the dye in the final solid thin film.

Table 4. The optical properties of Coumarin 334 and Pyromethene 580

Source: Previous work of IBM summer students Brian Triplett and Eric Green

Dye	Chemical name	Molecular weight	Absorption max (nm)	Emission max (nm)	Color
Coumarin 334	2,3,5,6-1H,4H-Tetrahydro-9-acetylquinolizone-[9,91,1-gh]-coumarin	283.33	450 nm in EtOH	495nm	Green
Pyromethene 580	4,4-Difluoro-2,6-din-butyl-1,3,5,7,8-pentamethyl-4-bora-3a,4a-diaza-s-indacene	376.34	519nm in EtOH	550nm	Yellow green

It is assumed that all the DCE solvent liquid is evaporated after spin casting and post baking. The concentration of coumarin 334 in the thin film is expressed as:

$$[C334]=\frac{W_{C334}}{W_{C334}+W_{Py580}+W_{PMMA}}$$

The concentration of pyrromethene 580 in the thin film is defined as:

$$[Py580]=\frac{W_{Py580}}{W_{C334}+W_{Py580}+W_{PMMA}}$$

Where, W_{C334} , W_{Py580} , and W_{PMMA} are the weights of coumarin 334, pyrromethene 580, and PMMA, respectively.

For example, to make a 2% C334 specimen with particular concentrations of Py580 samples two steps are required:

- a) Mix the target amount of C334 in the 10% PMMA base solution to make 2% C334 stock solution
- b) Mix the target amount of Py580 powder in the 2% C334 stock solution to make specific two-dye concentration solution.

Using the above method, total six groups of specimens were prepared:

- 2% C334 with Py580 concentration ranging from 0 ~ 1% at an increment of about 0.1%.
- 4% C334 with Py580 concentration ranging from 0 ~ 1% at an increment of about 0.1%.

- 8% C334 with Py580 concentration ranging from 0 ~ 1% at an increment of about 0.1%.
- 0.1% Py580 with C334 concentration ranging from 0 ~ 10% at an increment of about 1%.
- Low concentration of Py580 ranging from 0 ~ 1% at an increment of about 0.1%.
- 4% C334 and 0.4% Py580 dye-pair specimens were used for the stability experiment.

4.2.3. Casting thin film

C334/Py580/PMMA solution was cast onto the surface of round quartz substrates (2.54cm-diameter and 0.5 mm thickness) by spin coating. The spin rate was 3000RPM.

Then the quartz plates were baked at 120°C for 15minutes on a hot plate in a N₂ gas flow. The thickness of a single layer thin film produced under this condition is about 1 μm.

For low concentration specimens, in order to increase the absorption of the incident light, the spin rate was lowered to 1500RPM; and the number of the layers increased to 3 layers. That is, the cast and spin steps are repeated three times, each cycle concluded with baking 120°C for 15 minutes in N₂ gas flow.

4.3 Color converter thin film optical properties measurement

4.3.1 UV Absorption measurement

The optical density (OD) of the thin film was measured by a Perkin Elmer Model Lambda 9 UV/VIS/NIR Spectrometer under room temperature and atmosphere. The

thickness of the thin film was measured by Alpha-step 200. Dividing the measured OD by thickness, the OD (in units of μm^{-1}) is obtained.

4.3.2 PL quantum efficiency measurement

The PL quantum efficiency for every concentration specimen was measured using the modified measurement method. (Section 3.8 and see setup in Fig.12). The incident light is the stimulated laser generated by a High Power Argon Ion Laser Model 2030 with a wavelength at 459nm. The PL spectra were taken by the Acton-Research SpectruMM Photoluminance Spectrometer with a CCD. Newport Model 818-SL power meters were used as the detector for the intensity of the incident, reflect and transmit light.

4.4 Degradation experiment for the two-dye system

To investigate the environmental degradation of the two-dye system, four groups of identical specimen (4% C334 with 0.4% Py580) were prepared. Each group consisted of two specimens. The specimens were stored at four different conditions. Table 5 indicates the storage condition for each group.

The PL quantum efficiency of the specimens stored at condition A (Table 5) was measured every day for the first week and every three days thereafter. An aging curve presenting the decaying PL quantum efficiency with time was obtained. The PL quantum efficiency for the specimens stored under condition B, C and D were measured after an accumulated exposure of two weeks.

Table 5. Exposure conditions for aging experiment

Condition	Light condition	Atmosphere
A	Florescent light	Air
B	Dark	Air
C	Florescent light	N₂
D	Dark	N₂

5. Results and Discussion

5.1 Optical properties of the coumarin 334 host dye

To investigate the relationship between the optical properties and dye concentration of the C334 one-dye system, a group of thin film specimens with the same thickness (about 1 μ m) but different C334 concentration (1% to 10% wt percent) was studied. The UV absorption and photoluminance quantum efficiency was measured. The influence of concentration effects on the absorption and quantum efficiency of the C334 one-dye system is summarized in Table 6 and Table 7.

5.1.1 Absorption

The UV absorption spectra of the C334 one-dye system with different concentrations are shown in Fig.17. There is a very slight shift in maximum absorbance wavelength with increased dye concentration from 446nm at 0.5% to 435nm at 11.8% (see Fig.18) and a small change in shape for the spectra. These observations indicate that the ground-state interactions between C334 molecules are weak. The trend of the maximum optical density as a function of C334 concentration is shown in Fig.19. Fig.19 shows the absorption of the thin film to be linearly dependent on the concentration of the dye. The linear curve of absorption vs. dye concentration suggests that the absorption behavior of C334 dye for concentrations to 10% in a thin film with PMMA matrix agrees with Beer's Law. The extinction coefficient for C334 in PMMA dilute thin film is $3.74 \times 10^4 \text{ (M}^{-1} \text{ cm}^{-1}\text{)}$.

Table 6 Concentration effect of C334 on the absorbance for one-dye system

Concentration of C334 (wt%)	Optical density at maximum wavelength	Maximum wavelength (nm)	Thickness (um)
0.5	0.1296	446	1.407
1.17	0.3006	446	1.39
1.45	0.3352	445	1.344
1.83	0.4567	445	1.34
3.51	0.8598	444	1.474
5.6	1.3153	441	1.505
7.18	1.6835	439	1.525
8.96	2.056	436	1.496
11.6	2.687	435	1.474

Table 7. Concentration effect of C334 on the quantum efficiency for one-dye system

Concentration of C334 (%)	Quantum efficiency (%)	Mean value of quantum efficiency (%)	Standard deviation
1.1	62.04	61.37	1.31
	62.65		
	59.63		
	61.15		
2.04	28.67	30.41	1.40
	31.78		
	31.26		
	29.93		
2.4	24.51	26.67	2.87
	23.90		
	28.69		
	29.56		
3.07	20.73	20.11	1.83
	18.29		
	19.03		
	22.38		
4.4	12.90	13.29	2.02
	15.96		
	11.06		
	13.23		
5.2	10.34	11.51	1.66
	12.98		
	9.84		
	12.89		
6.42	12.70	10.85	2.21
	11.02		
	13.3		
	8.45		
7.6	8.77	10.43	2.39
	11.79		
	7.14		
	12.54		
8.1	10.25	8.595	2.66
	9.49		
	7.65		
	11.75		
9.1	8.39	9.04	0.58
	9.55		
	8.69		
	9.51		
9.8	11.06	8.73	2.06
	8.36		
	9.77		
	8.96		

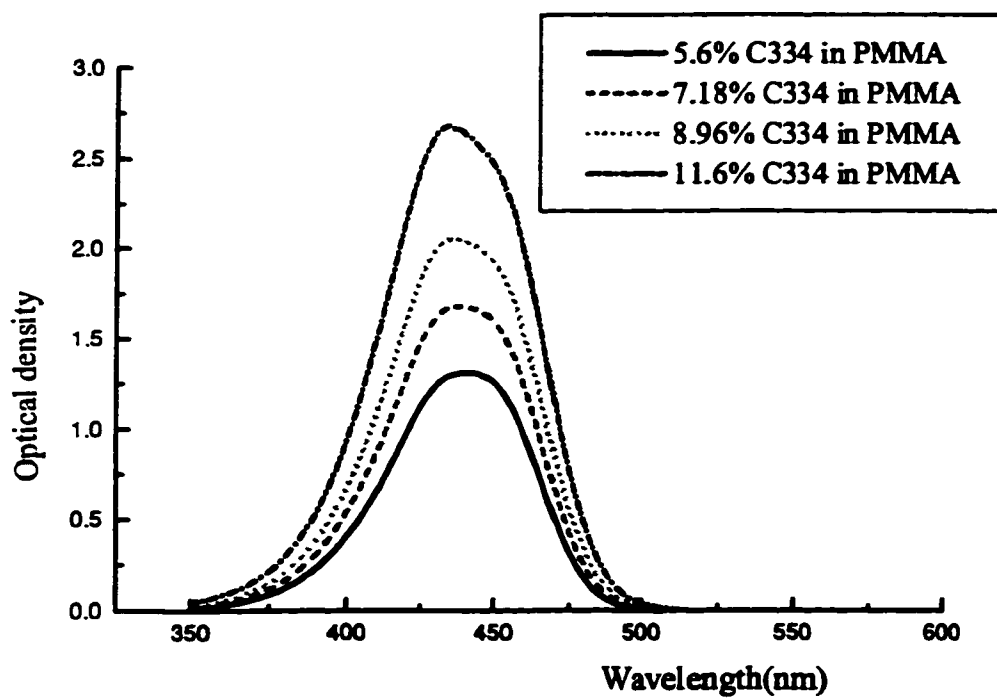
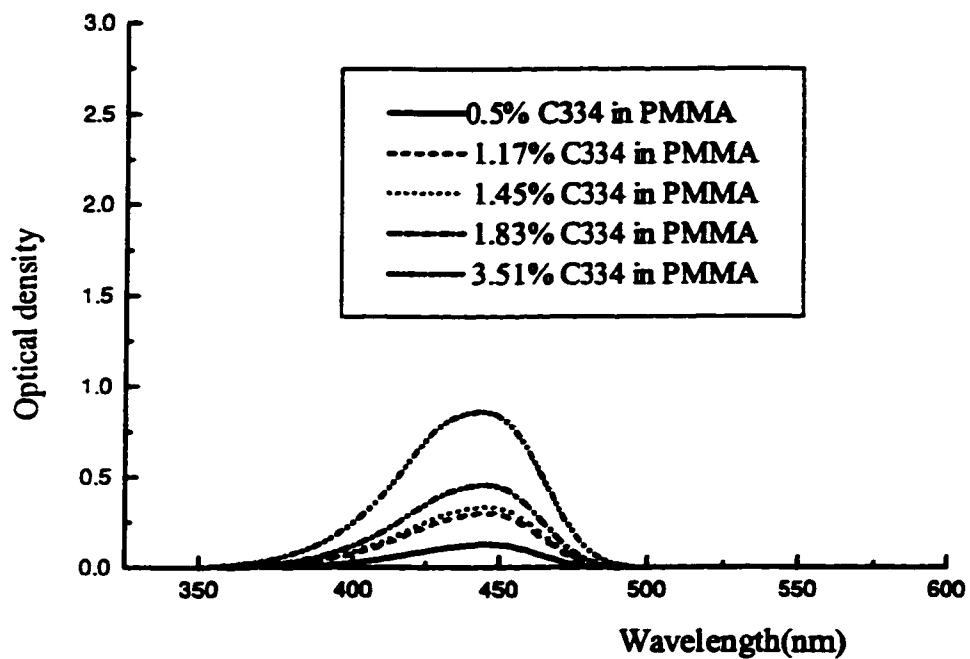


Fig.17 UV absorption spectra for various concentrations of C334 in PMMA matrix (Film thickness: 1.4 μ m)

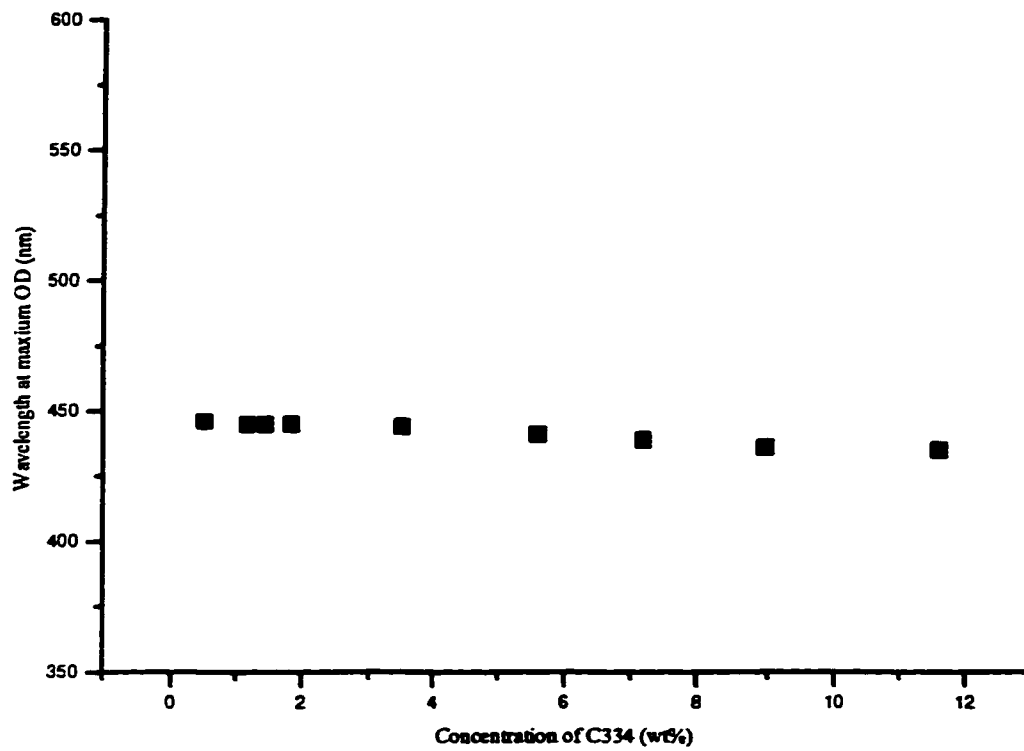


Fig.18 Shift of the maximum absorption wavelength with C334 concentration

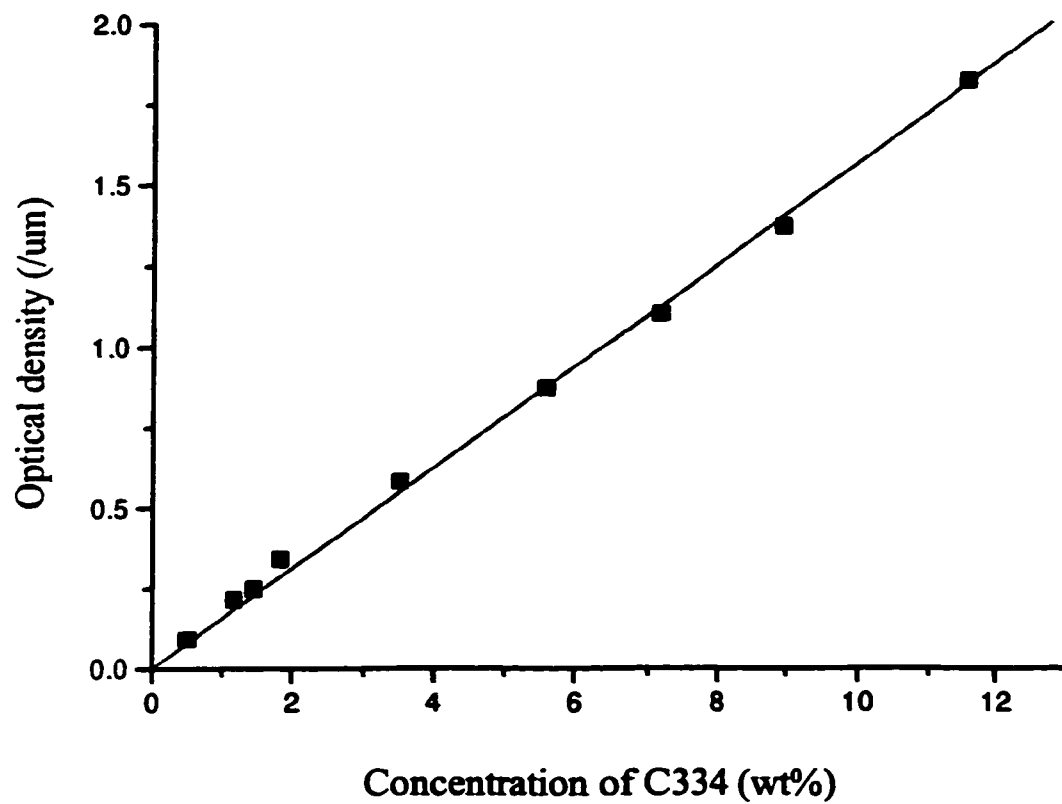


Fig.19 Optical density vs. C334 concentration for the C334 in PMMA matrix one-dye system (Film thickness: 1.4μm)

5.1.2 Photoluminance (PL) quantum efficiency

Fig.20 shows the photoluminance spectra of C334 as a function of concentration. Fig.21 is a trend curve of the PL quantum efficiency as a function of C334 concentration and is based on the data of Fig.20. Fig.21 illustrates that the PL quantum efficiency decreases with an increase of dye concentration. The Py580 one dye system shows the same trend (See Fig.22). The decreasing quantum efficiency with increasing dye concentration can be explained by concentration quenching. At high concentration, the excited dye molecule can interact with an unexcited dye molecule and form an excited dimer. The excited dimer relaxes at an inefficient non-radiative manner, which results in reduced PL quantum efficiency. The shift of PL maximum wavelength (Fig.23) is also an indication of excited state interaction.

Fig.24 shows the calculated brightness based on the data of Fig.19 and Fig.21 as a function of C334 concentration. It confirms the hypothesis (Section 3.6.4) that one dye cannot provide high absorption and high quantum efficiency concurrently to give the optimized brightness. Use of a two-dye system approach to color conversion for the OLED application is justified.

5.2 Two-dye system (Coumarin 334 and Pyrromethene 580 in PMMA)

To obtain the high absorption and high PL quantum efficiency concurrently, a second dye (guest dye) is introduced in the color converter and the two-dye (C334 with Py580) system is created. The PL spectra of the 3.99% C334 one dye system and 3.99% C334 with 0.036% Py580 two-dye system are compared in Fig.25.

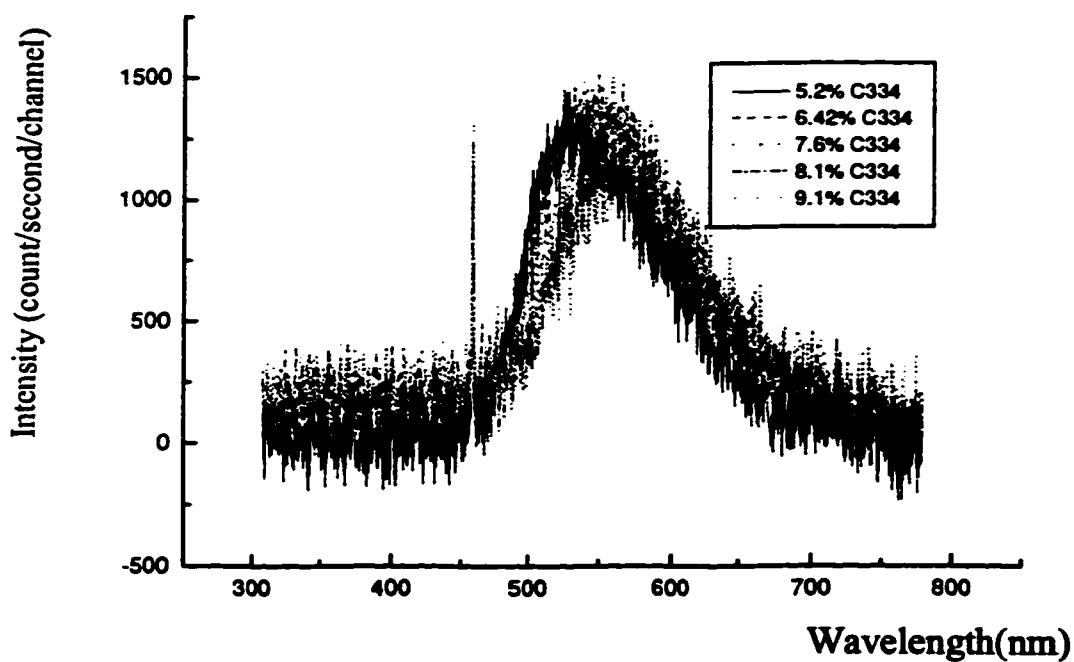
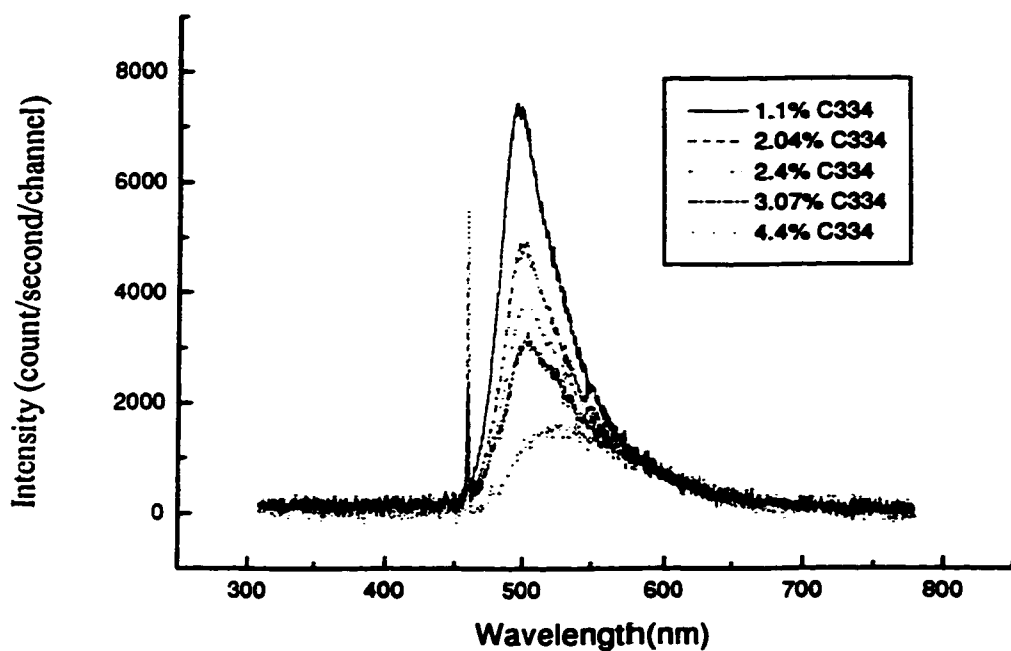


Fig.20 PL Spectra for different concentration of C334 in PMMA matrix one-dye system
Illumination source: 459nm laser
Film thickness: 1.4um

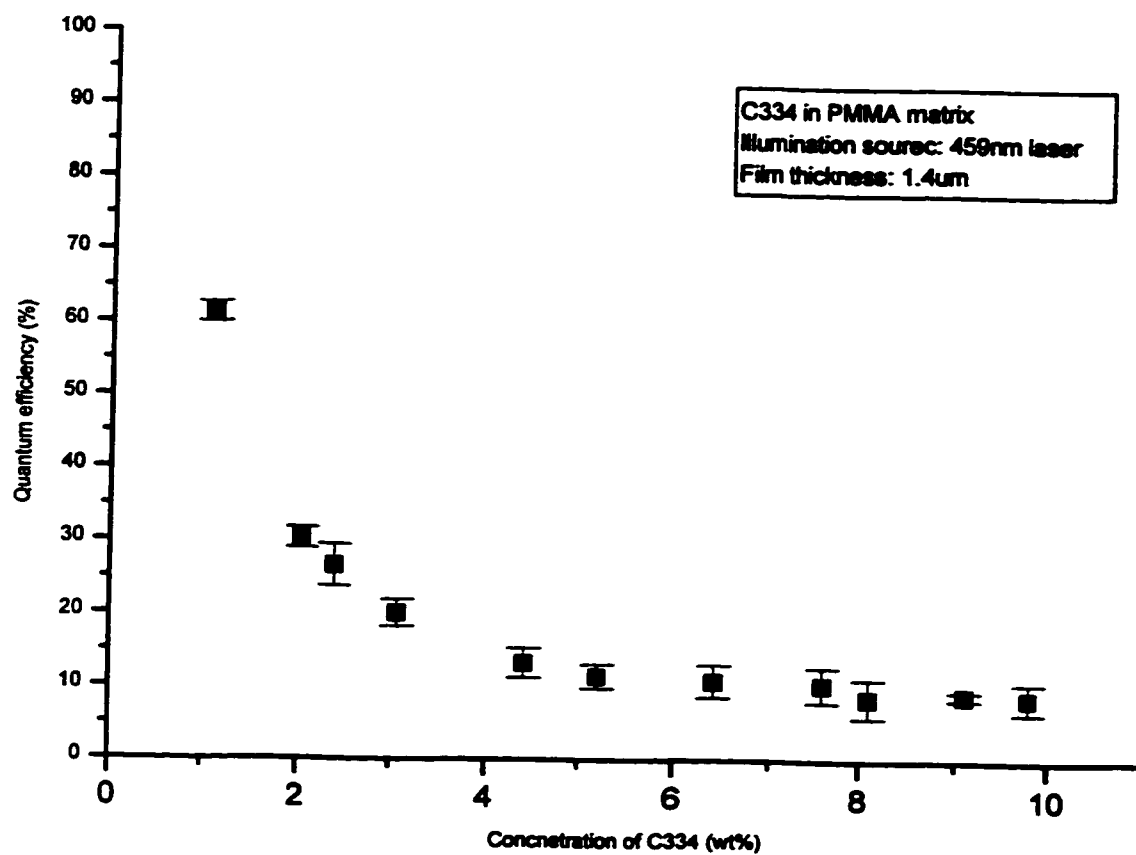
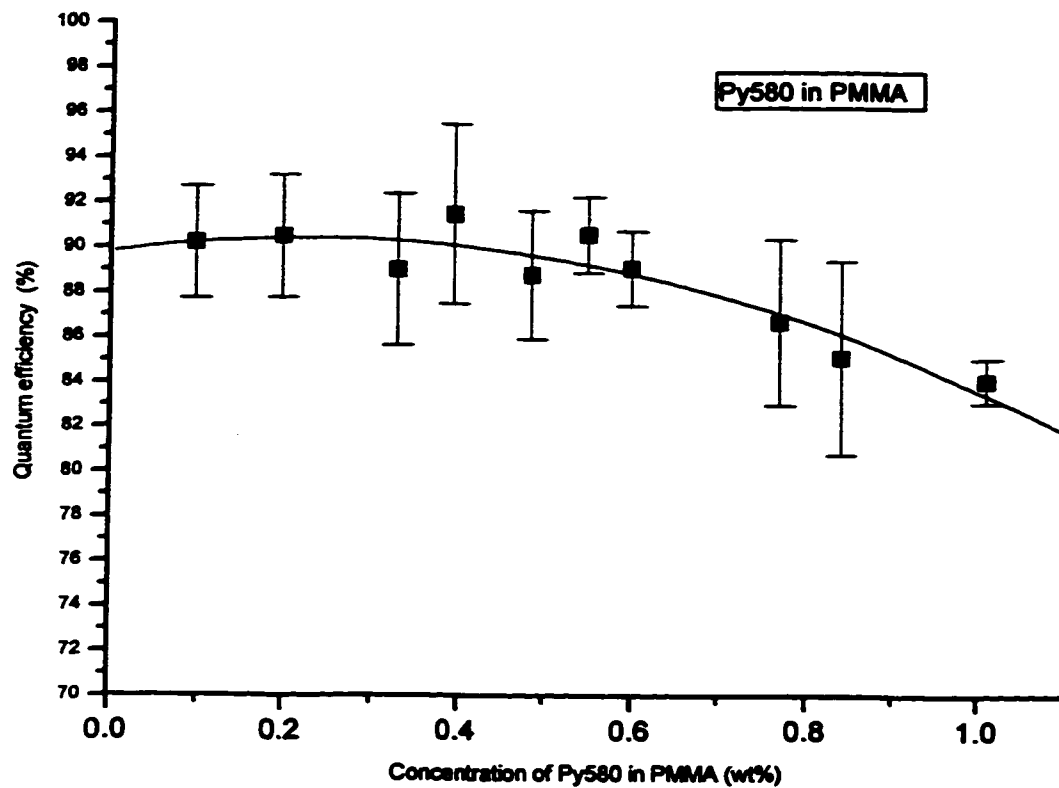


Fig.21 Concentration influence on the quantum efficiency for C334 one-dye system



**Fig.22 Concentration effect of Py580 on PL quantum efficiency for Py580 in PMMA matrix one dye system
Illumination source: 459nm laser
Film thickness: 1.4um**

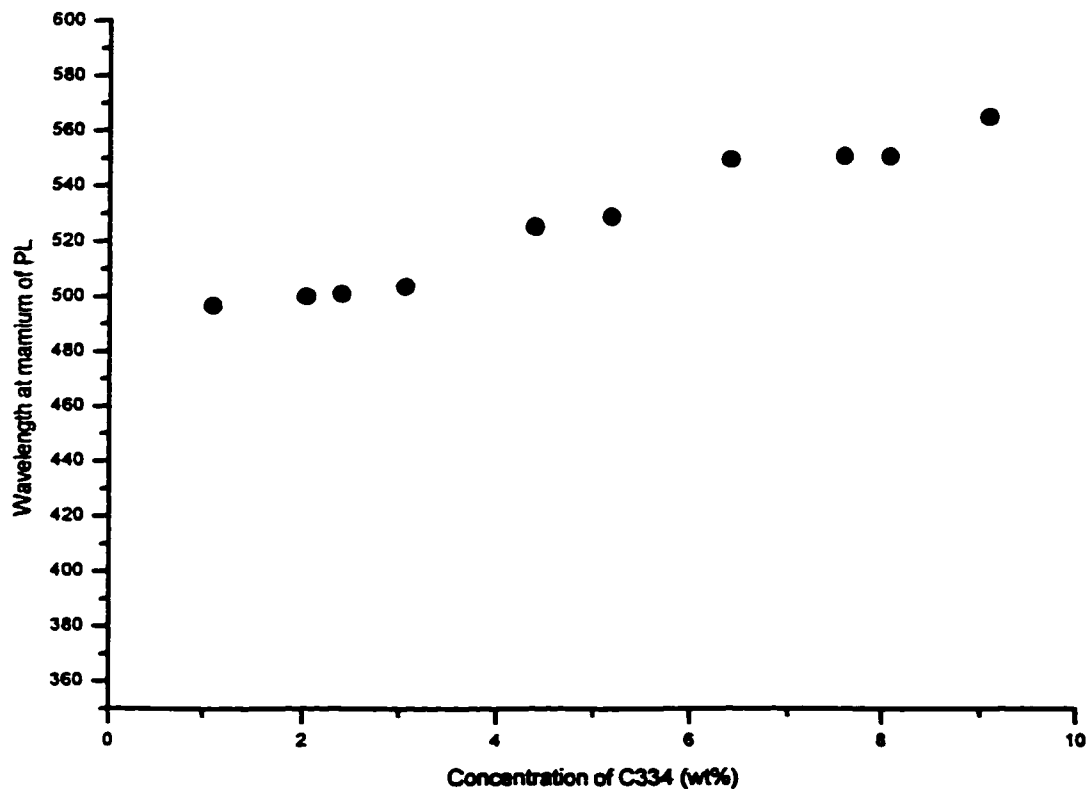


Fig.23 Drift of the PL wavelength maximum as a function of C334 concentration

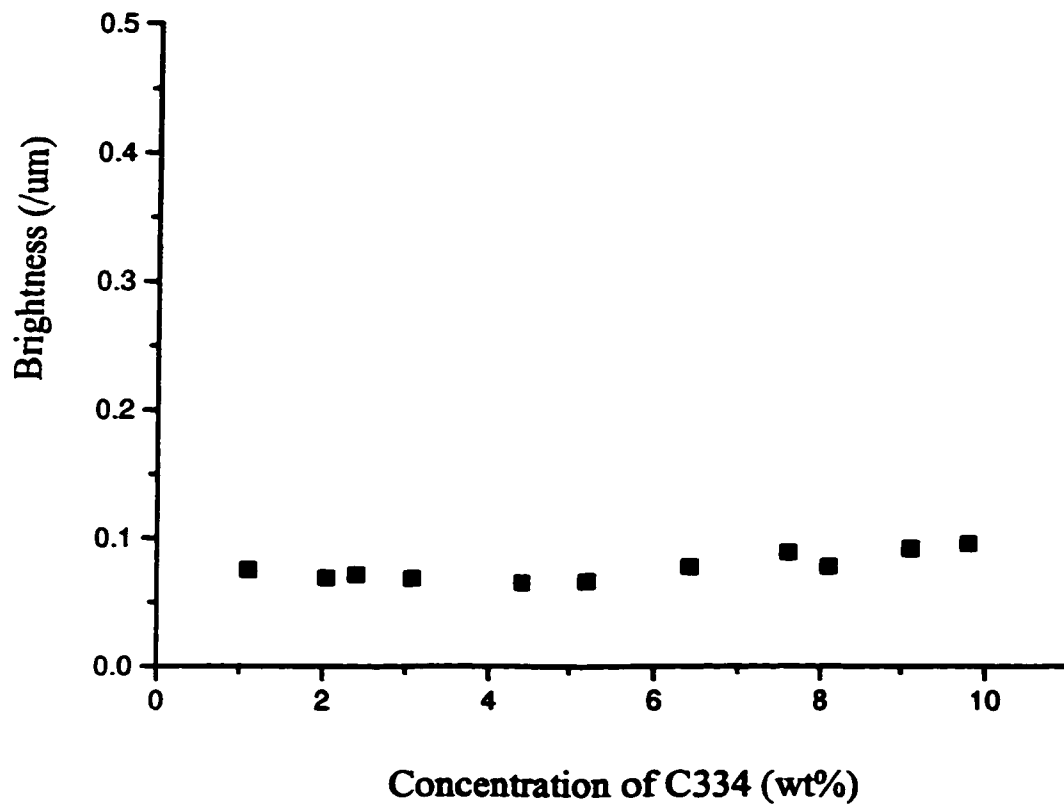
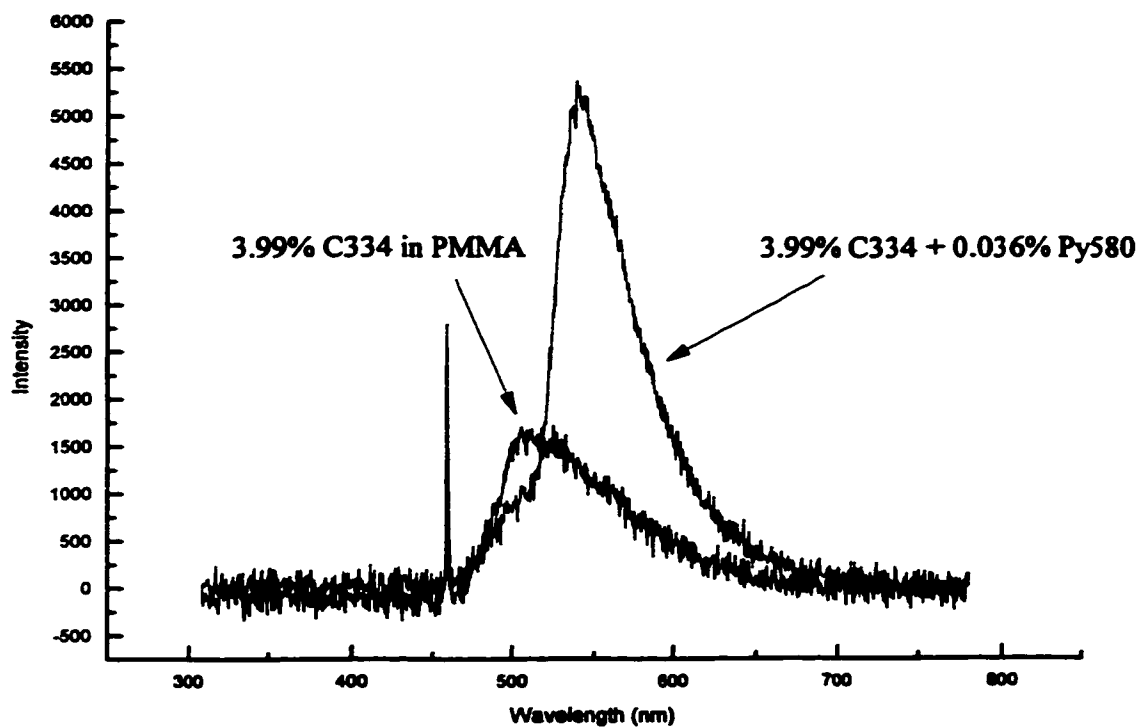


Fig.24 Brightness for C334 one-dye system as a function of C334 concentration



**Fig.25 PL spectra of 3.99% C334 in PMMA matrix and
3.99% C334 with 0.036% Py580 in PMMA matrix
Illumination source: 459nm laser
Film thickness: 1.4um**

The excitation wavelength of the stimulating laser is 459nm. In the C334 one-dye system, the maximum emission wavelength is 505nm, which is the emission wavelength of C334. With a small amount (0.036% wt percent) of Py580 introduced, the maximum emission wavelength shifts to 544nm. This is the emission wavelength of Py580. Also the emission intensity of the two-dye system (over 5000 counts/second/channel in peak intensity) is much higher than the one-dye system. The data confirm that C334 (host dye) absorbs the laser light efficiently and transfers energy to Py580 (guest dye). Radiative transition from guest dye results. This is what is expected of a two-dye system.

5.2.1 Concentration influence of the dye-pair on the PL quantum efficiency

To study the concentration effect of each of the dyes on the PL quantum efficiency for a two-dye system, three groups of thin film specimens were made. Each group had a fixed C334 concentration (2%, 4% or 8%) by weight. Within each host group, the concentration of Py580 (guest dye) was varied. The concentration of Py580 ranged from 0.1% to 1%. Table 8, Table 9, and Table 10 record the optical measurements. The PL quantum efficiency dependence on the dye-pair concentration is summarized in Fig.26, where concentrations of 2%, 4%, and 8% C334 are represented. From the trend curves of Fig.26, the following are observed:

(1) The introduction of a very small amount of guest dye (less than 0.1%) increases the PL quantum efficiency dramatically (from 30% to 70% for the 2% C334 with 0.1% Py580) in the two-dye system.

Table 8 Concentration effect for 2% C334 + Py580 in PMMA (DCE)

Concentration of C334 (%)	Concentration of Py580 (%)	Quantum efficiency (%)	Mean value of quantum efficiency (%)	Standard deviation
1.99	0	29.95	30.87	2.4
		28.32		
		34.00		
		31.20		
1.99	0.074	69.60	69.91	1.48
		69.98		
		71.82		
		68.24		
1.988	0.179	70.54	73.34	2.75
		71.91		
		74.06		
		76.85		
1.985	0.335	76.69	77.05	0.8
		78.63		
		77.92		
		77.75		
1.982	0.485	77.94	79.97	3.5
		79.79		
		84.99		
		77.15		
1.98	0.554	82.26	80.84	2.85
		84.06		
		79.32		
		77.73		
1.976	0.795	75.88	73.48	2.38
		70.45		
		74.77		
		72.83		
1.973	0.84	71.19	73.38	1.98
		74.22		
		75.69		
		72.41		
1.973	0.94	75.73	72.08	3.73
		68.23		
		74.79		
		69.58		
1.968	1.17	64.11	67.13	3.13
		69.97		
		69.69		
		64.75		

Table 9 Concentration effect of 4% C334 + Py580

Concentration of C334 (%)	Concentration of Py580 (%)	Quantum efficiency (%)	Mean value of quantum efficiency (%)	Standard deviation
3.99	0	10.46	10.79	0.77
		10.30		
		10.46		
		11.94		
3.99	0.036	21.55	22.80	1.10
		22.31		
		23.30		
		24.06		
3.987	0.135	46.79	45.84	1.86
		45.37		
		43.45		
		47.73		
3.99	0.2	50.24	50.01	2.08
		47.01		
		51.13		
		51.66		
3.98	0.25	53.96	52.10	2.19
		50.00		
		54.04		
		50.41		
3.98	0.31	51.70	50.11	1.759
		51.56		
		48.60		
		56.13		
3.977	0.386	52.44	52.62	2.73
		49.46		
		52.46		
		53.12		
3.97	0.53	51.51	51.875	1.23
		50.32		
		52.55		
		51.80		
3.964	0.695	49.77	48.46	2.83
		45.66		
		46.64		
		42.03		
3.957	0.874	47.73	46.67	3.192
		49.33		
		47.59		

Table 10 Concentration effect for 8% C334 + Py580 in PMMA (DCE) on PL quantum efficiency

Concentration of C334 (%)	Concentration of Py580 (%)	Quantum efficiency (%)	Mean value of quantum efficiency (%)	Standard deviation
8.04	0.11	19.77	20.08	1.14
		18.93		
		19.98		
		21.66		
8.03	0.208	26.29	25.47	1.37
		26.06		
		26.11		
		23.42		
8.03	0.26	32.02	8.03	0.26
		33.06		
		32.36		
8.02	0.41	36.14	34.5	3.38
		30.5		
		38.21		
		33.13		
8.01	0.52	37.27	37.67	0.568
		37.89		
		38.37		
		37.15		
8.00	0.578	35.07	36.5	1.83
		34.98		
		38.82		
		37.1		
8.00	0.68	33.27	33.9	1.76
		36.48		
		33.51		
		32.45		
7.99	0.815	28.42	29.9	2.7
		33.98		
		28.46		
		28.81		
8.03	0.98	23.01	25.4	1.712
		26.86		
		26.4		
		25.33		

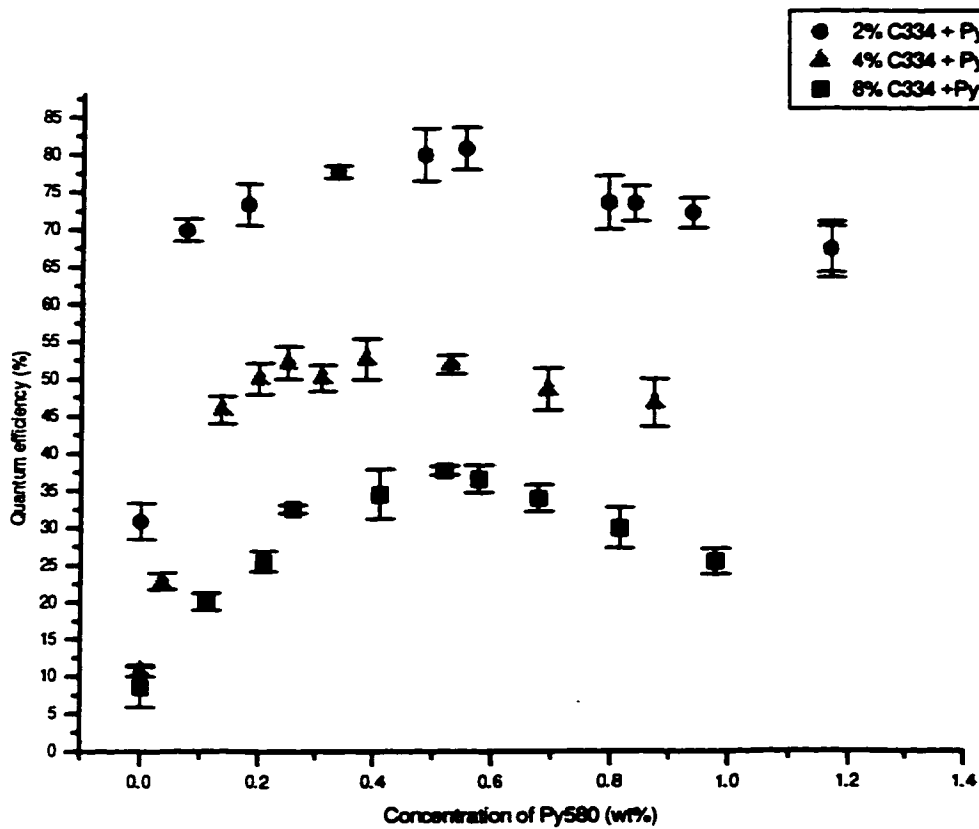


Fig.26 Dye pair Concentration influence on the PL quantum efficiency for C334 + Py580 two-dye system
Illumination source: 459nm laser
Film thickness: 1.4um

(2) PL quantum efficiency strongly depends on the concentration of the host dye. The greater the concentration of the host dye, the lower the quantum efficiency. There is a fall in PL quantum efficiency from a maximum about 80% for the 2% C334 group to about 35% for the 8% C334 group. The measurements of PL quantum efficiency for various concentrations of C334 with fixed concentration of Py580 (Fig.27) support the same conclusion. When the Py580 concentration is fixed at 0.1%, the PL quantum efficiency drops with the increasing C334 Concentration. Fig.28 shows the brightness dependence on the concentration of C334 with 0.1% Py580. The brightness of the two-dye system is optimized at a C334 concentration of around 6%.

(3) For this two-dye system, beyond some threshold guest dye concentration, the PL quantum efficiency is weakly dependent on the concentration of the guest dye. There is a maximum PL quantum efficiency around 0.5% Py580 concentration irrespective of the host dye concentration for the range of the dye concentrations investigated.

5.2.2 Data analysis with energy transfer model

In order to understand the observed data trends of Fig.26 in terms of the energy transfer mechanism of the two-dye system, the energy transfer characteristics based on the Forster energy transfer model are considered.

For the one-dye system, the energy absorbed by dye molecules can be released in one of two ways: non-radiative and radiative [i.e. via fluorescence emission (see Fig.29)]. The fraction of radiated energy released, $F(r)$, is equal to the PL quantum efficiency by definition.

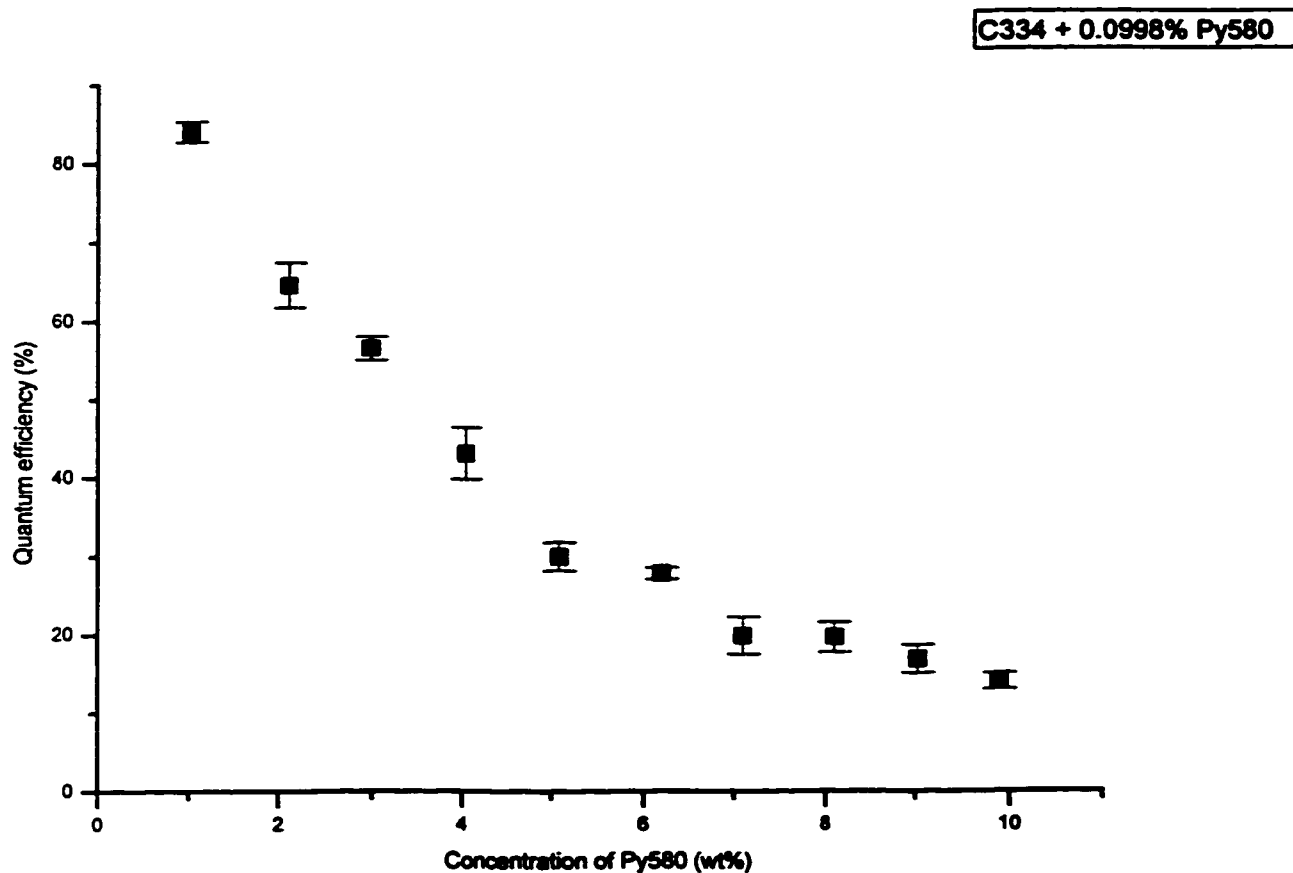


**Fig.27 PL quantum efficiency dependency on various concentrations of C334 (host dye) with fixed concentration (0.1%) of Py580
Illumination source: 459nm laser
Film thickness: 1.4um**

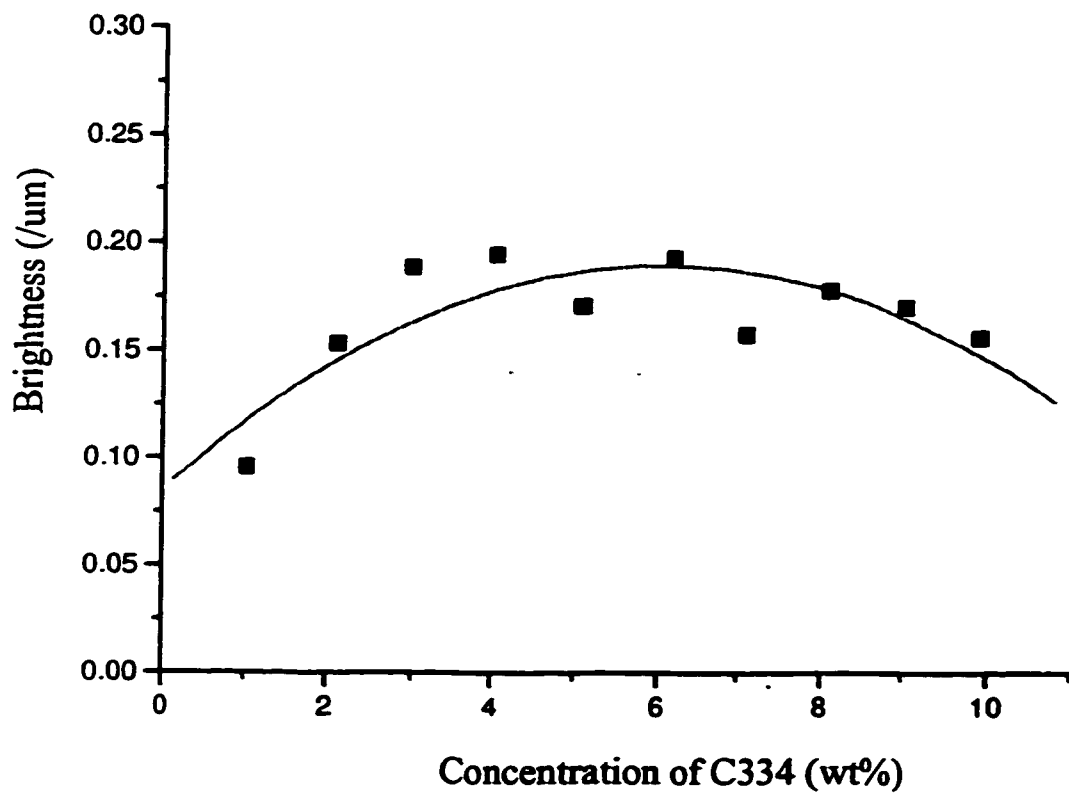


Fig.28 The brightness of various concentration of C334 with 0.1% Py580 in PMMA (Film thickness: 1.4μm)

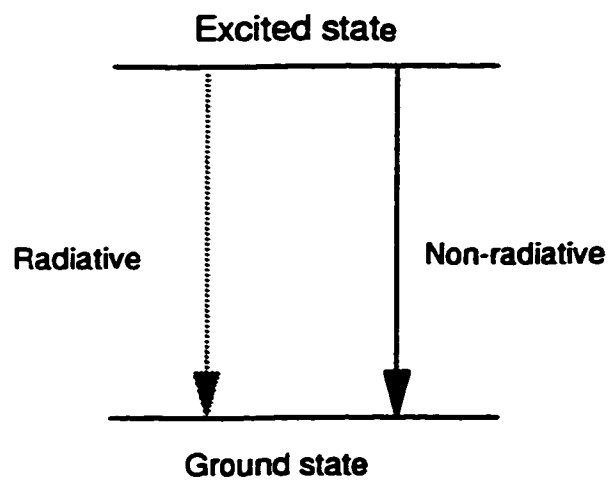


Fig.29 One-dye system energy release model

So

$$F(r)_{C334} = \Phi_{C334} \quad (\text{Eq.21})$$

$$F(nr)_{C334} = 1 - \Phi_{C334} \quad (\text{Eq.22})$$

$$F(r)_{Py580} = \Phi_{Py580} \quad (\text{Eq.23})$$

$$F(nr)_{Py580} = 1 - \Phi_{Py580} \quad (\text{Eq.24})$$

Where, Φ_{C334} : PL quantum efficiency of C334 one dye system at certain concentration

Φ_{Py580} : PL quantum efficiency of Py580 one dye system at certain concentration

$F(r)_{C334}$: The fraction of absorbed energy radiated by C334

$F(nr)_{C334}$: The fraction of absorbed energy released by C334 via non-radiative transition

$F(r)_{Py580}$: The fraction of absorbed energy released by Py580 via radiative transition.

$F(nr)_{Py580}$: The fraction of absorbed energy released by Py580 via non-radiative transition.

For the two-dye system, the basic energy transfer and release model is illustrated in Fig.30. Part of the absorbed energy can be released by the host dye with both radiative and non-radiative components. The rest of the absorbed energy is transferred to the guest dye, then eventually released by radiative and non-radiative mechanisms. The sum of $F(r)_{C334}$ and $F(r)_{Py580}$ must be equal to the PL quantum efficiency measured for the two-dye system.

$$F(r)_{C334} + F(r)_{Py580} = \Phi_{C334 + Py580} \quad (\text{Eq.25})$$

$$F(nr)_{C334} + F(nr)_{Py580} = 1 - \Phi_{C334 + Py580} \quad (\text{Eq.26})$$

Here $\Phi_{C334 + Py580}$ is the PL quantum efficiency of the C334 with P580 two-dye system at certain concentration.

Also

$$F(r)_{C334} = \Phi_{C334} \times \eta \quad (\text{Eq.27})$$

Where η is the ratio of the energy released by C334 in the two-dye system to the energy released by C334 in the C334 one-dye system. The value of η can be estimated by comparing the intensity at 505nm (the peak emission wavelength for C334) in the one dye system and the intensity of C334 with Py580 the two-dye system at the same position (505nm). This is illustrated in Fig.31, where BC is the 505nm intensity for the two-dye system and AC is the 505nm intensity for the one-dye system. So $\eta = BC/AC$

Substitute Eq.27 in Eq.25, one gets:

$$F(r)_{Py580} = \Phi_{C334 + Py580} - F(r)_{C334} \quad (\text{Eq.28})$$

It is assumed that the energy transferred to the guest dye is only released by the guest dye as fluorescent radiation and that secondary non-radiative energy loss does not occur. So

$$\frac{F(r)_{Py580}}{F(nr)_{Py580}} = \frac{\Phi_{Py580}}{1 - \Phi_{Py580}} \quad (\text{Eq.29})$$

Rearranging Eq.29, one gets

$$F(nr)_{Py580} = \frac{1 - \Phi_{Py580}}{\Phi_{Py580}} \times F(r)_{Py580} \quad (\text{Eq.30})$$

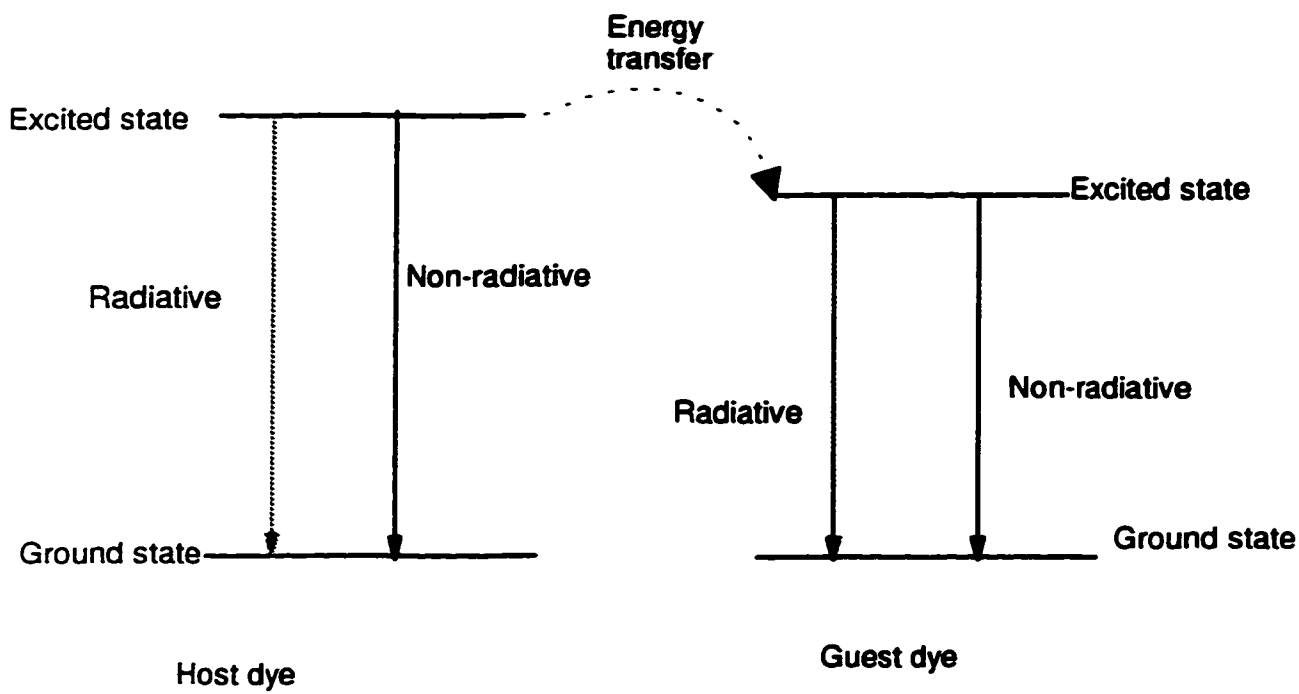


Fig.30 Two-dye system energy transfer and release model

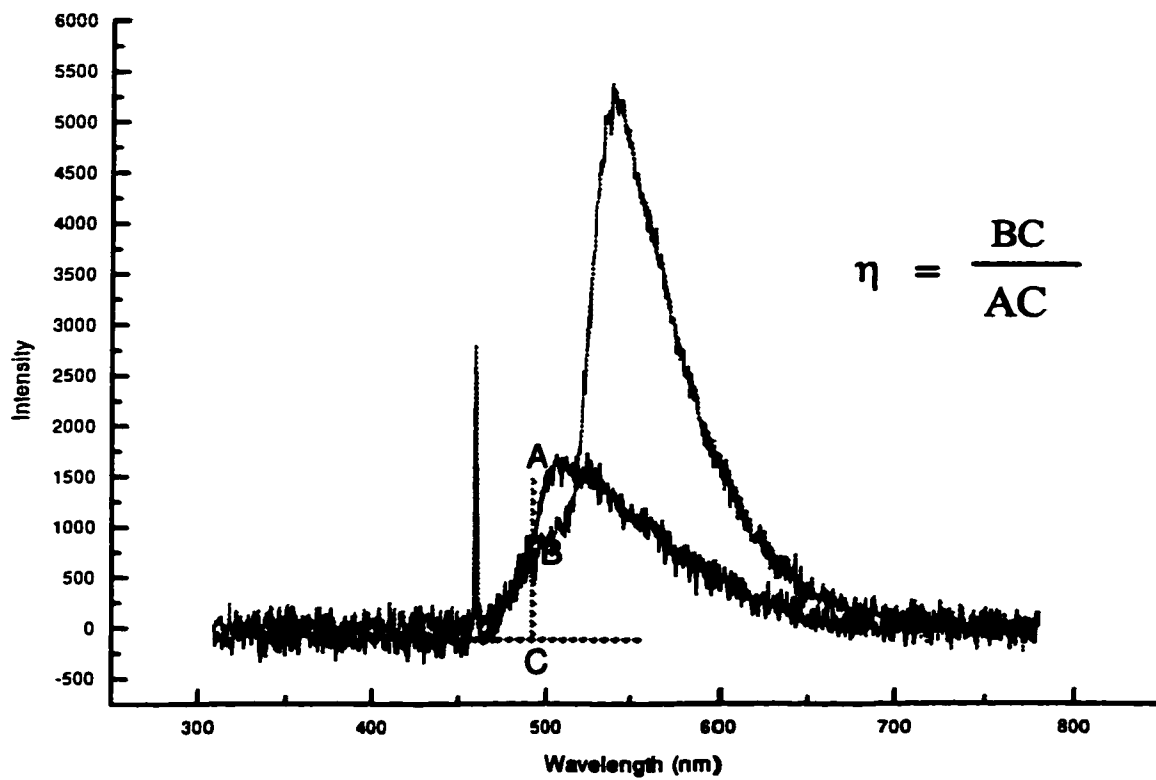


Fig.31 Illustration of the definition of η

In summary, the fraction of radiative and non-radiative components for both the host and guest dyes are:

$$F(r)_{C334} = \Phi_{C334} \times \eta \quad (\text{Eq.31})$$

$$F(r)_{Py580} = \Phi_{C334 + Py580} - \Phi_{C334} \times \eta \quad (\text{Eq.32})$$

$$F(nr)_{Py580} = \frac{1 - \Phi_{Py580}}{\Phi_{Py580}} \times F(r)_{Py580} \quad (\text{Eq.33})$$

$$F(nr)_{C334} = 1 - F(r)_{C334} - F(r)_{Py580} - F(nr)_{Py580} \quad (\text{Eq.34})$$

The energy flows calculated by the above method when applied to the data of Fig.26 are shown in Fig.32 and Fig.33 (for 2% C334 with Py580 and 4% C334 with Py580, respectively). The model suggests that most of the absorbed energy released by Py580 is radiative and by is C334 non-radiative in two-dye system. The radiative relaxation in the guest dye competes with non-radiative fluorescence in the host dye. The latter increases with host dye concentration and therefore limits the overall PL quantum efficiency.

5.2.3 Color purity of the C334/Py580 two-dye system

The CIE coordinate number for 3.98% C334 with 0.39% Py580 is (0.41, 0.56), a color point located within the yellow-green area in the CIE chromaticity diagram. The purity (Pe) is quite high at 0.94.

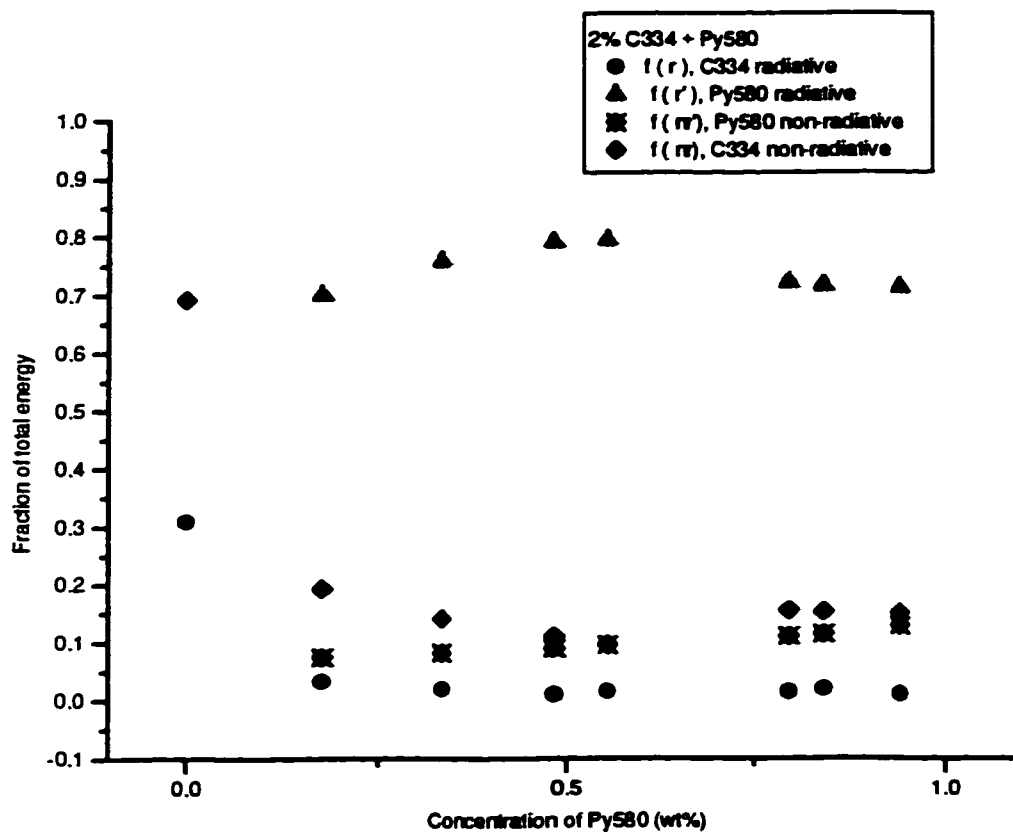


Fig.32 Energy flow for 2% C334with Py580 in PMMA matrix

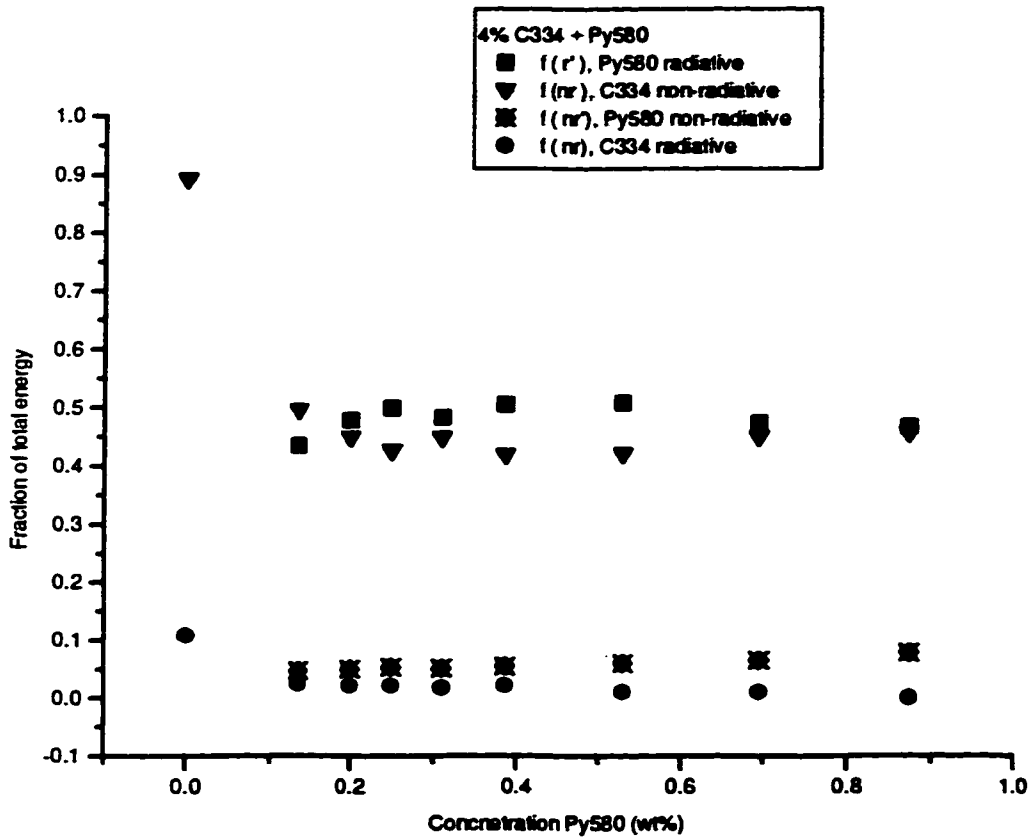


Fig.33 Energy flow for 4% C334 with Py580 in PMMA matrix

5.2.4 The storage stability of the C334/ Py580 two-dye system

The environmental decay in the PL quantum efficiency for the 2.84% C334 with 0.54% Py580 in PMMA matrix, two-dye system is shown in Fig.34. Table11 records the PL quantum efficiency of the four groups of specimens stored at the specified conditions. Based on the measurements, the following can be concluded:

- 1. The quantum efficiency of the C334/Py580/PMMA color converter system decayed when exposed to air and light concurrently. The PL quantum efficiency rapidly drops about 16-percentage points (from 59.86% to 43.18%) in 48 hours. Then the PL quantum efficiency drops only 4-percentage points in the following 200 hours. Indeed, a plateau in PL quantum efficiency decay may be exhibited. More data would be required to address this possibility.**
- 2. Table 11 shows that the C334/Py580 two-dye system color converter degrades when exposed to fluorescent light in the presence of O₂ or N₂. Without fluorescent light there is no decay. It suggests that the mechanism is photo-degradation.**

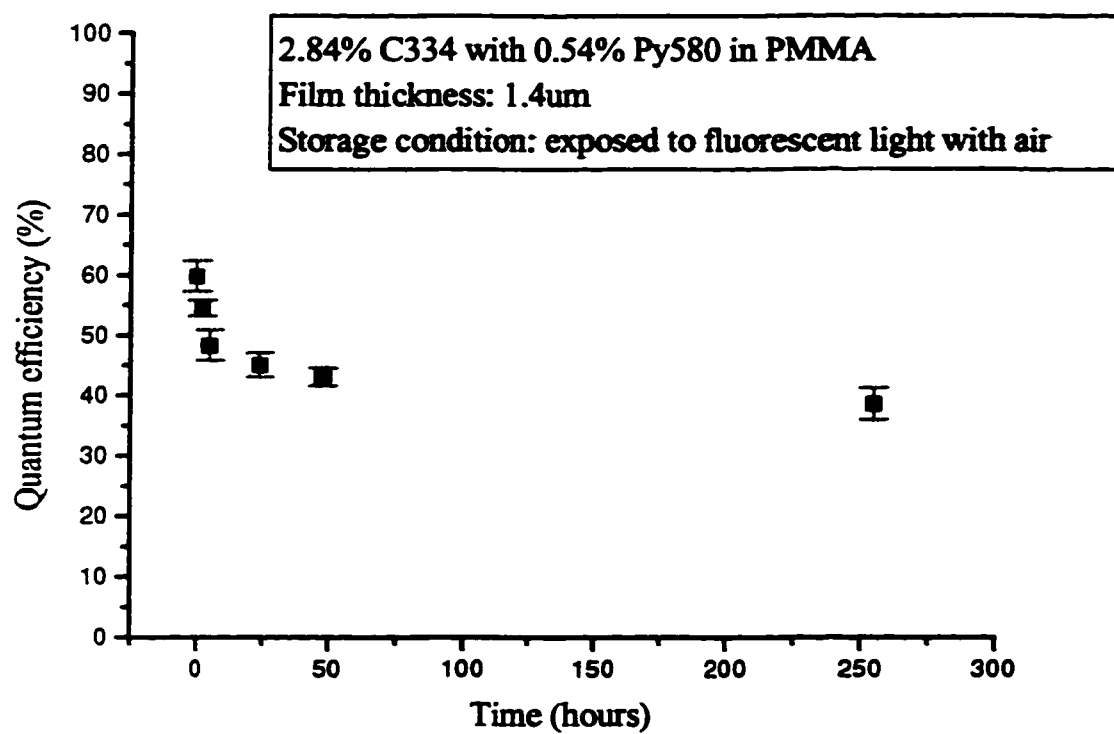


Fig.34 The PL quantum efficiency decay for the C334/Py580 two-dye system
Illumination source: 459nm laser

**Table 11. PL quantum efficiency comparison for C334/Py580 two-dye system
stored at different conditions**

Time	Storage condition			
	O ₂ /light	O ₂ /dark	N ₂ /light	N ₂ /dark
Starting point	59.86%±2.57%			
Ending point (after 11 days)	38.65%± 2.64%	59.97%±1.35%	60.02%±1.2%	37.25%±1.06%

6. Conclusions

From the reported results, the following conclusions can be drawn.

- 1. Both the absorbance and the PL quantum efficiency of Coumarin 334 single dye system are dye-concentration dependent. The higher the dye concentration, the higher the optical density (OD), and the lower the PL quantum efficiency. That is, opposite trends are observed.**
- 2. Use of the two-dye system for color converter is justified to obtain the concurrent high absorbance and PL quantum efficiency. With 0.1% Pyrromethene 580, the two-dye system has optimized brightness when the concentration of Coumarin 334 is approximately 6%. Additionally, the PL quantum efficiency resulting from the energy transfer inherent in the two-dye system increases from 30% to 70% for 2% C334 with addition of 0.1% Py580.**
- 3. The PL quantum efficiency of C334/Py580/PMMA two-dye system is strongly dependent on the host dye concentration and weakly dependent on the guest dye concentration.**
- 4. In the two-dye system, about 90% of the absorbed energy is released via radiative relaxation by the guest dye and non-radiative relaxation by the host dye. These two mechanisms compete with each other. The non-radiative fluorescence increases with the increase of host dye concentration and therefore the overall PL quantum efficiency decreases.**
- 5. The C334/Py580 two-dye system is unstable when exposed to fluorescent light in the presence of O₂ or N₂. The likely mechanism is photo-degradation.**

References

1. Tasch, S., C. Brandstatter, F. Meghdadi, and G. Leising, "Red-Green-Blue Light Emission from a Thin Film Electroluminescence Device Based on Parahexaphenyl," *Advanced Materials* (September 1997): 33.
2. Gu, G., and Stephen R. Forrest, "Design of Flat-Panel Displays Based on Organic Light-Emitting Devices," *IEEE Journal of Selected Topics in Quantum Electronics* 4, No.1 (1998): 83.
3. Service, Robert F., "Organic Light Emitters Gain Longevity," *Science* 273 (August 1996): 878-880.
4. Web site <http://www.universaldisplay.com/apps.html>
5. Shoustikov, Andrei A., Yujian You, and Mark E. Thompson, "Electroluminescence Color Tuning by Dye Doping in Organic Light-Emitting Diodes," *IEEE Journal of Selected Topics in Quantum Electronics* 4, No. 1 (1998): 1077.
6. Helfrich, W., and W. G. Schneider, "Recombination Radiation in Anthracene Crystals," *Phys. Rev. Lett.* 14 (1965): 229-231.
7. Hosokawa, C., M. Matsuura, M. Eida, K. Fukuoka, H. Nakamura, and T. Kusumoto, "Organic Multicolor EL Display with Fine Pixels," *Journal of the SID* (1997): 331.
8. Scott, J. Campbell, and George G. Malliaras, *The Chemistry, Physics and Engineering of Organic Light-Emitting Diodes*, Weinheim: Wiley-VCH, 1999, in press.
9. Web site <http://www.bway.net/~jscruggs/notice2.html>
10. Burrows, P. E., G. Gu, V. Bulovic, Z. Shen, S. R. Forrest and M. E. Thompson, "Achieving Full-Color Organic Light-Emitting Devices for Lightweight, Flat-Panel Displays," *IEEE Transactions on Electron Devices* 44, No.8 (August 1997): 1188.
11. Parker, Cecil. A., *Photoluminescence of Solutions*, New York: Elsevier publishing company, 1968, 19.
12. de Mello, John C., H. Felix Wittmann, and Richard H. Friend, "An Improved Experimental Determination of External Photoluminescence Quantum Efficiency," *Advanced Materials* 9, No.3 (1997): 230-232.

13. Wu, Chung-Chih, James C. Sturm, Richard A. Register, Jing Tian, Elena. P. Dana, and Mark E. Thompson, "Efficient Organic Electroluminescent Devices using Single-Layer Doped Polymer Thin Films with Bipolar Carrier Transport Abilities," *IEEE Trans. Electron Devices* 44 (1997): 1269-1279.
14. Birks, John B., *Photophysics of Aromatic Molecules*, London: Wiley-Interscience, 1970.
15. Luque, A., and E. Lorenzo, "Conditions for Achieving Ideal and Lambertian symmetrical Solar Concentrations," *Applied Optics* 20, No.21 (1982): 3736.
16. Ranby, B. and J. F. Rabek, *Photodegradation, photo-oxidation and photostabilization of polymers*, New York: John Willey & Sons, 1975, 97.